J. Fluid Mech. (2014), vol. 747, pp. 605–634.
doi:10.1017/jfm.2014.166

Geostrophic adjustment with gyroscopic waves: stably neutrally stratified fluid without the traditional approximation

G. M. Reznik†

P. P. Shirshov Institute of Oceanology, Russian Academy of Sciences, 36, Nakhimovskiy Prospekt, 117997, Moscow, Russia

(Received 12 July 2013; revised 5 January 2014; accepted 21 March 2014; first published online 23 April 2014)

We examine nonlinear geostrophic adjustment in a rapidly rotating (small Rossby number Ro) stably neutrally stratified (SNS) fluid consisting of a stratified upper layer with $N > f$ (N is the buoyancy frequency, f the Coriolis parameter) and a homogeneous lower layer, the density and other fields being continuous at the interface between the layers. The angular speed of rotation is non-parallel to gravity; the traditional and hydrostatic approximations are not used. The wave spectrum in the model consists of internal and gyroscopic waves. During the adjustment an arbitrary long-wave perturbation is split in a unique way into slow quasi-geostrophic (QG) and fast ageostrophic components with typical time scales $(Ro f)^{-1}$ and f^{-1}, respectively. The QG flow is governed by two coupled nonlinear equations of conservation of QG potential vorticity (PV) in the layers. The fast component is a sum of internal waves and inertial oscillations (long gyroscopic waves) confined to the homogeneous layer and modulated by an amplitude depending on coordinates and slow time. On times $t \sim (f Ro)^{-1}$ the slow component is not influenced by the fast one but the inertial oscillations amplitude is coupled to the QG flow and obeys an equation practically coinciding with that in the barotropic case (Reznik, *J. Fluid Mech.*, vol. 743, 2014, pp. 585–605). A non-stationary boundary layer with large vertical gradients of horizontal velocity develops in the stratified layer near the interface to prevent penetration of the inertial oscillations into the stratified fluid; an analogous weaker boundary layer arises near the upper rigid lid. At large times the internal waves gradually decay because of dispersion and the resulting motion consists of the slow QG component and inertial oscillations confined to the barotropic lower layer.

Key words: rotating flows, stratified flows, waves in rotating fluids

1. Introduction

Reznik (2014) examined nonlinear geostrophic adjustment with gyroscopic waves of a barotropic fluid rotating at a constant angular speed $\boldsymbol{\Omega}$ non-parallel to gravity. The rotation was assumed to be rapid (the Rossby number $Ro = U/f L$ is small) and the motion to be large scale (the horizontal scale L greatly exceeds the fluid layer depth H); here U is the typical horizontal velocity and $f = 2\Omega \sin\varphi$ (see figure 1) is

† Email address for correspondence: greznikmd@yahoo.com

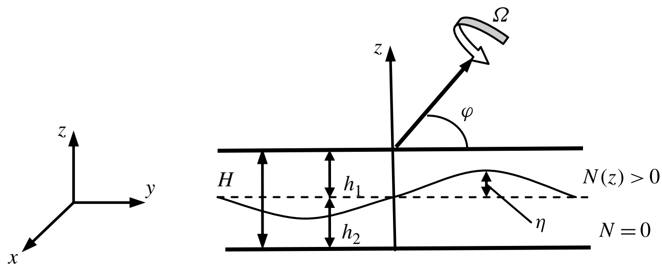

FIGURE 1. Schematic representation of rotating stably neutrally stratified fluid.

the Coriolis parameter. It was shown that an arbitrary perturbation is split in a unique way into slow and fast components evolving with characteristic time scales $(Rof)^{-1}$ and f^{-1}. Equations governing each of the components were derived and analysed. The slow component does not depend on depth and is close to the geostrophic balance. On times $O(1/f\,Ro)$ the slow component is not influenced by the fast one and obeys the two-dimensional fluid dynamics equation for a geostrophic streamfunction. The fast component consists of long gyroscopic waves and is a packet of inertial oscillations modulated by an amplitude depending on coordinates and slow time. The horizontal component of twice the angular speed $f_s = 2\Omega \cos\varphi$ was not assumed to be zero and neither the traditional approximation (TA) nor the hydrostatic approximation were used.

In this work we generalize these results to the case of a stratified fluid. In stratified fluid under the TA ($f_s = 0$) sub-inertial gyroscopic waves coexist with super-inertial internal waves only under the condition $N_{min} < f$ where N_{min} is the minimal value of the buoyancy frequency N (e.g. Kamenkovich 1977); in strongly stratified fluid, i.e. for $N_{min} > f$, only super-inertial internal waves are possible. Here we consider a stably neutrally stratified (SNS) fluid which is the simplest model where gyroscopic and internal waves coexist together. The fluid consists of stratified upper layer with $N > f$ and homogeneous lower layer, the density and other fields being continuous at the interface between the layers. The configuration is of practical interest since recent observations indicate that, at least in some parts of the world's oceans, there exist practically homogeneous or very weakly stratified (i.e. with $N \leqslant f$) near-bottom layers several hundred metres thick (e.g. van Haren & Millot 2005; Timmermans, Melling & Rainville 2007).

Reznik (2013) examined the linear dynamics of SNS fluid with and without rotation. A special feature of the system is the wave mode related to the homogeneous layer. In non-rotating fluid this is the zero-frequency homogeneous layer vortex mode related to conservation of three-dimensional vorticity in the homogeneous layer. In the mode a steady three-dimensional velocity field is confined to the homogeneous layer, and at the interface between the layers the vertical velocity is zero and the horizontal velocity can be discontinuous. The discontinuity results in a non-stationary boundary layer arising near the interface at large times that prevents penetration of a stationary signal into the upper stratified layer. Besides this mode, the wave spectrum also contains internal waves and the zero-frequency horizontal vortex mode with zero vertical velocity.

In rotating SNS fluid the horizontal and homogeneous layer vortex modes turn into the geostrophic mode and gyroscopic waves, respectively. The wave spectrum of the system has been examined by taking into account the horizontal component of the angular speed of the Earth's rotation, i.e. without the traditional and hydrostatic approximations. The spectrum combines sub-inertial gyroscopic waves in the homogeneous fluid (e.g. LeBlond & Mysak 1978; Brekhovskikh & Goncharov 1994) and internal and internal inertio-gravity waves in the stably stratified fluid (Badulin, Vasilenko & Yaremchuk 1991; Kasahara 2003; Gerkema & Shrira 2005; Gerkema *et al.* 2008).

The paper is organized as follows. In § 2 the governing equations of SNS fluid are given. In § 3 a geostrophic mode in the system is examined and long internal and gyroscopic waves are briefly discussed. Section 4 contains non-dimensional equations and an asymptotic procedure for finding the solution. The lowest-order solution as a sum of a quasi-geostrophic (QG) component, internal waves and modulated inertial oscillations located in the lower layer is represented in § 5; special attention is paid to analysis of non-stationary boundary layers arising near the interface and upper rigid lid. In § 6 the first-order solution is analysed and slow evolution of the QG flow and inertial oscillations is described. Section 7 contains a discussion and conclusions. Some technical details of calculations are given in appendices A–G.

2. Governing equations

We consider a fluid layer of constant depth H, bounded by two rigid lids and rotating as a whole at a constant angular speed $\boldsymbol{\Omega}$ which, generally, is not parallel to gravity (directed along the z-axis in figure 1). To provide in a simple way for the coexistence of internal and gyroscopic waves (i.e. the condition $N_{min} < f$) we assume that the fluid density ρ, being continuous, depends on the depth z in the upper layer of depth $h_1 - \eta$ and is constant in the lower layer of depth $h_2 + \eta$ where h_1 and $h_2 = H - h_1$ are constant mean depths of the layers and $\eta = \eta(x, y, t)$ is the perturbation of interface between the layers (see figure 1).

Correspondingly, the density ρ and pressure p in the layers are given by the formulae:

$$\rho = \begin{cases} \rho_s(z) + \rho', & 0 \geqslant z \geqslant -h_1 + \eta \\ \rho_0 = \text{const.}, & -h_1 + \eta \geqslant z \geqslant -H; \end{cases} \tag{2.1a}$$

$$p = \begin{cases} g\displaystyle\int_z^0 \rho_s \mathrm{d}z + p', & 0 \geqslant z \geqslant -h_1 + \eta \\ -g\rho_0(z + h_1) + g\displaystyle\int_{-h_1}^0 \rho_s \mathrm{d}z + p', & -h_1 + \eta \geqslant z \geqslant -H, \end{cases} \tag{2.1b}$$

where $\rho_s = \rho_s(z)$ is the upper layer density at the rest state, the equilibrium density being continuous, i.e. $\rho_s(-h_1) = \rho_0$; ρ', p' are the variations of density and pressure from their hydrostatic profiles.

Motion of the fluid obeys the following equations:

$$\boldsymbol{u}_t + \boldsymbol{u}\cdot\nabla\boldsymbol{u} + 2\boldsymbol{\Omega}\times\boldsymbol{u} + \boldsymbol{e}_z g\rho/\rho_0 = -\nabla p'/\rho_0, \tag{2.2a}$$

$$\rho_t + \boldsymbol{u}\cdot\nabla\rho - \rho_0 N^2 w/g = 0, \quad \nabla\cdot\boldsymbol{u} = 0 \tag{2.2b,c}$$

in the domain $0 \geqslant z \geqslant -h_1 + \eta$, and

$$\boldsymbol{u}_t + \boldsymbol{u}\cdot\nabla\boldsymbol{u} + 2\boldsymbol{\Omega}\times\boldsymbol{u} = -\nabla p'/\rho_0, \quad \nabla\cdot\boldsymbol{u} = 0 \tag{2.3a,b}$$

in the domain $-h_1 + \eta \geqslant z \geqslant -H$. Here $\boldsymbol{u} = (u, v, w)$ is the velocity; u, v, w are the velocity components along the x-, y-, z- axes, respectively; $2\boldsymbol{\Omega} = \boldsymbol{e}_y f_s + \boldsymbol{e}_z f$; g is the acceleration due to gravity; $\boldsymbol{e}_x$, $\boldsymbol{e}_y$, $\boldsymbol{e}_z$ are the unit vectors along corresponding axes; $N^2 = -g\partial_z\rho_s/\rho_0$. The prime in density variations is omitted and (assuming the variations to be small) the density is replaced by the constant value ρ_0 where it is not differentiated. At the rigid surface and bottom the velocity satisfies the no-flux condition:

$$w|_{z=0,-H} = 0. \tag{2.4a}$$

Conditions at the interface $z = -h_1 + \eta$ depend of the type of solution that is sought. The solution is assumed to be continuous with all derivatives in the domains above and below the interface, with a possible singularity at the interface itself. The simplest model of this kind taking into account effects of density stratification is a two-layer fluid with a constant upper layer density $\rho_1 < \rho_0$. However, the standard two-layer model does not describe the important property that the gyroscopic waves can be locked in weakly stratified domains and do not penetrate into strongly stratified ones (Reznik 2013). That is why in our model the upper layer is stably stratified.

The type of singularity at the interface depends on initial conditions. If at the initial moment the density and tangential velocity have a discontinuity and the normal velocity is continuous at the interface then the interface is a tangential discontinuity. Since the fluid is incompressible, the interface (see e.g. Kochin, Kibel & Rose 1964; Sedov 1997) is a material surface at which the continuity of pressure should be fulfilled. We, however, are interested in a more realistic regime when the density and velocity fields are continuous at the interface at the initial moment and remain continuous for all time. The continuity of fields prevents possible Kelvin–Helmholtz instability and makes it possible to study the ‘buffer’ zone between the stably stratified and homogeneous domains in which a non-stationary boundary layer can arise (Reznik 2013).

The density is conserved in the fluid elements so they cannot intersect the interface which, therefore, is a material surface at which the conditions

$$(\rho_s + \rho)_{z=-h_1+\eta} = \rho_0, \quad w|_{z=-h_1+\eta} = \eta_t + u\eta_x + v\eta_y \tag{2.4b,c}$$

should be fulfilled. The continuity of all fields means that in addition to (2.4b,c) the horizontal velocity and pressure also are continuous at $z = -h_1 + \eta$:

$$[u]_{z=-h_1+\eta} = 0, \quad [v]_{z=-h_1+\eta} = 0, \quad [p]_{z=-h_1+\eta} = 0; \tag{2.4d–f}$$

here and below $[a]_{z=z_0} = a|_{z=z_0+0} - a|_{z=z_0-0}$. We note that the continuity of horizontal velocity together with (2.4c) provide the continuity of the vertical velocity w. The continuity of pressure (2.4f) together with (2.1b) implies for the pressure deviation p':

$$[p']_{z=-h_1+\eta} = g\int_{-h_1}^{-h_1+\eta} (\rho_s - \rho_0)\mathrm{d}z. \tag{2.4g}$$

Finally, the initial conditions can be written as:

$$(u, v, \rho)_{t=0} = (u_I, v_I, \rho_I)(x, y, z); \quad w_I = -\int_{-H}^{z} (\partial_x u_I + \partial_y v_I)\mathrm{d}z; \tag{2.4h,k}$$

here and below the subscript ‘I’ denotes initial fields.

The problem (2.2), (2.3) and (2.4) seems to be overdetermined since three conditions of continuity (2.4d–f) are used instead of one condition of continuity of pressure as in the case of tangential discontinuity. It turns out, however, that the conditions (2.4*d–f*) are not independent as will be seen from the perturbation analysis below: the continuity of pressure together with continuity of initial velocity fields guarantees the continuity of the fields all the times.

We emphasize that the continuity of the fields does not imply continuity of their derivatives. If the derivatives (of any order) are discontinuous at $z=-h_1+\eta$ then the interface is a so-called weak discontinuity. Details of the theory of weak discontinuities can be found in Kochin *et al.* (1964). For example, if the buoyancy frequency $N(z)$ is not zero at $z=-h_1$, i.e.

$$N(-h_1)\neq 0, \tag{2.5}$$

then the interface is a weak discontinuity, since the physical fields here are continuous but their gradients are discontinuous. In some calculations below we will use the simplest configuration with a weak discontinuity when the background upper layer density profile $\rho_s(z)$ linearly depends on z and N is a constant, i.e.

$$\rho_s=-\frac{\rho_0}{g}N^2(z+h_1)+\rho_0. \tag{2.6}$$

It follows from (2.4*b*), (2.6) that in this case

$$\rho|_{z=-h_1+\eta}=\frac{\rho_0}{g}N^2\eta; \tag{2.7}$$

the formula relates density perturbation at the interface to perturbation of the interface. Also using (2.4*g*) and (2.6) one can find a jump of pressure variation across the interface $z=-h_1+\eta$:

$$[p']_{z=-h_1+\eta}=-\frac{\rho_0}{2}N^2\eta^2. \tag{2.8}$$

3. Linear modes

In this section we consider linear modes in the system (2.2), (2.3). The wave spectrum consists of gyroscopic, internal and internal inertio-gravity waves with non-zero frequency and a zero-frequency geostrophic mode. The non-zero frequency waves were examined in detail in Reznik (2013) and here only the case when stratification is strong, $f/N_0\ll 1$ (N_0 is the characteristic buoyancy frequency), and the waves are long, $L\gg H$, is briefly discussed in § 3.1. Here and below L is the horizontal scale of motion. The geostrophic mode is considered in § 3.2 without restrictions on the stratification and scales.

3.1. *Long gyroscopic and internal waves*

The linearized version of (2.2), (2.3) can be reduced to two equations for the vertical velocity w (e.g. Miropol'sky 2001):

$$(\partial_{tt}+f^2)w^+_{zz}+\nabla_h^2 w^+_{tt}+2ff_s w^+_{yz}+f_s^2 w^+_{yy}+N^2\nabla_h^2 w^+ = 0, \tag{3.1a}$$

$$(\partial_{tt}+f^2)w^-_{zz}+\nabla_h^2 w^-_{tt}+2ff_s w^-_{yz}+f_s^2 w^-_{yy} = 0, \tag{3.1b}$$

where $\nabla_h^2=\partial_{xx}+\partial_{yy}$. Boundary conditions for (3.1*a*) and (3.1*b*) follow from (2.4*a,c,d,e*) and the continuity equations (2.2*c*), (2.3*b*):

$$w^+|_{z=0}=w^-|_{z=-H}=0,\quad [w]=[w_z]=0. \tag{3.2a,b}$$

Here and below the superscripts + and − denote quantities in the upper and lower layers, respectively; $[a]=a^+|_{z=-h_1}-a^-|_{z=-h_1}$.

The wave solutions

$$w^{\pm}=W^{\pm}(z)\exp[\mathrm{i}(kx+ly-\sigma t)]+\mathrm{c.c.} \tag{3.3}$$

to (3.1), (3.2) were examined in detail in Reznik (2013). Here we are interested in the physically important scale range

$$H \ll L \leqslant L_R, \tag{3.4}$$

where $L_R = HN_0/f$ is the Rossby scale. Neglecting small terms in (3.1) gives the following approximate equations:

$$(\partial_{tt}+f^2)w^+_{zz}+N^2\nabla_h^2 w^+=0, \quad (\partial_{tt}+f^2)w^-_{zz}=0. \tag{3.5a,b}$$

The wave spectrum of the system (3.5), (3.2) consists of super-inertial internal waves (3.3) with $\sigma > f$ and inertial oscillations with $\sigma = f$. Amplitudes $W^{\pm}(z)$ of the internal wave obey the equations

$$W^+_{zz}+q^2W^+=0, \quad W^-_{zz}=0, \quad q^2=\frac{\kappa^2N^2}{\sigma^2-f^2}, \tag{3.6a–c}$$

where $\kappa=\sqrt{k^2+l^2}$. In the case (2.6) of constant N the solution to (3.6a,b) satisfying the boundary conditions (3.2) is readily found:

$$W^+_n=-\sin q_n z/\sin q_n h_1, \quad W^-_n=(z+H)/h_2, \quad n=1, 2, \ldots. \tag{3.7}$$

Here $q_n=s_n/h_1$ where s_n is the nth root of the equation

$$s\cot s=-h_1/h_2. \tag{3.8}$$

The corresponding dispersion relation has the form:

$$\sigma_n=\sigma_n^{\mathrm{iw}}=\sqrt{f^2+\kappa^2h_1^2N^2/s_n^2}. \tag{3.9}$$

In accordance with (3.7) the vertical mode amplitude oscillates in the upper stratified layer and depends linearly on depth in the lower one.

For the inertial oscillations with $\sigma = f$ it follows from (3.5) that

$$w^+=0, \quad w^-=A_s(x, y, z)\sin f t+A_c(x, y, z)\cos f t; \tag{3.10}$$

here the amplitudes $A_{s,c}$ are arbitrary functions obeying the conditions:

$$A_{s,c}|_{z=-h_1}=\partial_z A_{s,c}|_{z=-h_1}=A_{s,c}|_{z=-H}=0. \tag{3.11}$$

Thus the inertial oscillations here are confined to the homogeneous lower layer and do not penetrate into the upper one.

The non-hydrostatic and 'non-traditional' terms neglected in (3.1) to derive (3.5) are of no importance for the internal waves but they affect the inertial oscillations (3.10) (see Reznik 2013 for more details). The terms transform the oscillations into sub-inertial long gyroscopic waves of 'standard' form (3.3) with the approximate dispersion relation:

$$\sigma_n = \sigma_n^{gw} = f - \frac{f_s h_2}{2n\pi}|l|, \quad n = 1, 2, \dots, \tag{3.12}$$

coinciding with the dispersion relation of sub-inertial long gyroscopic waves in barotropic fluid of depth h_2 (see Reznik 2014). In these waves the vertical mode amplitudes W_n oscillate in the lower layer and decay exponentially in the upper one with increasing distance from the interface. As follows from (3.9) and (3.12), in the scale range (3.4) the internal waves are strongly dispersive, whereas the gyroscopic ones are characterized by a weak dispersion.

It is seen from (3.9) and the above discussion that the gyroscopic (internal) waves become close to the inertial oscillations if $L \gg H (L \gg L_R)$. In the case $f/N_0 \ll 1$ the Rossby scale greatly exceeds the depth H, i.e. the gyroscopic waves make possible the inertial oscillations with $L \leqslant L_R$ which are shorter than the 'traditional' inertial oscillations related to the long internal modes from the scale range $L \gg L_R$. One can assume that this fact explains the large vertical velocities in inertial oscillations observed in the nearly barotropic deep Western Mediterranean (van Haren & Millot 2005).

3.2. *Geostrophic mode*

Besides the wave modes (3.3) there exists a zero-frequency geostrophic mode satisfying the linearized equations (2.2), (2.3) with the boundary conditions (2.4). This mode is related to conservation laws of potential vorticity (PV) which are conveniently derived using the new variables (cf. Reznik 2014):

$$x' = x, \quad y' = y - \alpha z, \quad z' = z. \tag{3.13}$$

With these variables the linearized problem (2.2), (2.3) is written in the form:

$$u_t^{\pm} - f v^{\pm} + f_s w^{\pm} = -p_{x'}^{\pm}, \quad v_t^{\pm} + f u^{\pm} = -p_{y'}^{\pm}, \tag{3.14a,b}$$

$$w_t^{\pm} - f_s u^{\pm} + g\rho^{\pm}/\rho_0 = -p_{z'}^{\pm} + \alpha p_{y'}^{\pm}, \quad \rho_t^{+} - (\rho_0 N^2/g) w^{+} = 0, \tag{3.14c,d}$$

$$u_{x'}^{\pm} + v_{y'}^{\pm} + w_{z'}^{\pm} - \alpha w_{y'}^{\pm} = 0. \tag{3.14e}$$

Here and below $\alpha = f_s/f$, $\rho^- = 0$, $p^{\pm} = p'^{\pm}/\rho_0$.

Elimination of the pressure $p^{\pm}$ from (3.14*a,b*) gives the vorticity equation:

$$(v_{x'}^{\pm} - u_{y'}^{\pm})_t - f w_{z'}^{\pm} = 0. \tag{3.15}$$

The stratified layer PV is obtained from (3.15) and (3.14*d*):

$$\Pi^{+} = v_{x'}^{+} - u_{y'}^{+} - (fg/\rho_0)(\rho^{+}/N^2)_{z'} = \Pi_I^{+}(x', y', z'). \tag{3.16}$$

To find an analogous invariant in the homogeneous layer we use the boundary condition at the interface (2.4*c*). With the variables (3.13) the equation for the interface becomes more complicated:

$$z' = -h_1 + \eta(x', y' + \alpha z', t). \tag{3.17}$$

However, in the linear approximation (3.17) takes the form $z' = -h_1 + \eta(x', y' - \alpha h_1, t)$, therefore the linearized condition (2.4*c*) can be written as

$$w|_{z'=-h_1} = \eta_t. \tag{3.18}$$

Integration of (3.15) over z' from $-H$ to $-h_1$ taking into account (3.18) and (2.4*a*) gives the PV in the homogeneous layer:

$$\Pi^- = \frac{1}{h_2}\int_{-H}^{-h_1} (v^-_{x'} - u^-_{y'})\,\mathrm{d}z' - \frac{f}{h_2}\eta = \Pi^-_I(x', y'). \tag{3.19}$$

The values $\Pi^\pm_I$ of the invariants are determined by the initial fields (2.4*h*) being equal to the left-hand sides of (3.16), (3.19) at the initial moment.

The potential vorticity in the SNS fluid is a 'hybrid' of those in a stratified fluid and in a barotropic fluid with a free surface. The upper layer PV (3.16) is a sum of the vertical component of relative vorticity and the term $-(fg/\rho_0)(\rho^+/N^2)_{z'}$ corresponding to the vortex-tube stretching between isopycnals (e.g. Pedlosky 1979). In the homogeneous layer PV equation (3.19) the first term is the depth-averaged relative vorticity and the term $-f\eta/h_2$ is the vortex-tube stretching due to perturbations of the interface.

The third invariant is the surface density $\rho^+|_{z'=0}$; in view of (3.14*d*) and the no-flux condition (2.4*a*) we have:

$$\rho^+|_{z'=0} = \rho^+_I|_{z'=0}. \tag{3.20}$$

As in the barotropic case (Reznik 2014), the solution to the problem (3.14) is represented as a sum of a geostrophic stationary part $(\boldsymbol{u}_g, \rho_g, p_g)$ with non-zero invariants $\Pi^\pm$, $\rho^+|_{z'=0}$ and an ageostrophic wave part $(\boldsymbol{u}_a, \rho_a, p_a)$ consisting of the harmonic waves (3.3) with non-zero frequencies and the zero invariants. One can readily show, using the bottom no-flux condition from (2.4*a*), that in the stationary solution the vertical velocity is zero and the lower layer motion does not depend on z':

$$u^\pm_g = -(1/f)\partial_{y'}p^\pm_g, \quad v^\pm_g = (1/f)\partial_{x'}p^\pm_g, \quad w^\pm_g = 0, \tag{3.21a–c}$$

$$\rho^\pm_g = -(\rho_0/g)\partial_{z'}p^\pm_g, \quad \partial_{z'}p^-_g = 0. \tag{3.21d,e}$$

The geostrophic pressure $p^\pm_g$ is determined using (3.16), (3.19):

$$\nabla'^2_h p^+_g + f^2(\partial_{z'}p^+_g/N^2)_{z'} = f\Pi^+_I(x', y', z'), \tag{3.22a}$$

$$\nabla'^2_h p^-_g - (f^2/h_2)\eta_g = f\Pi^-_I(x', y'), \tag{3.22b}$$

where $\nabla'^2_h = \partial_{x'x'} + \partial_{y'y'}$. Boundary condition at the surface $z' = 0$ follows from (3.20) and (3.21*d*):

$$\partial_{z'}p^+_g|_{z'=0} = -(g/\rho_0)\rho^+_I|_{z'=0}. \tag{3.23a}$$

The boundary condition for p^+_g at the interface is discussed in appendix A and can be written in a form suitable both for continuous $(N^2(-h_1) = 0)$ and discontinuous $(N^2(-h_1) \neq 0)$ buoyancy frequency profiles:

$$\lim_{z'\to -h_1}[(\partial_{z'}p^+_g/N^2)_{z'} - \partial_{z'}p^+_g/(h_2N^2)] = \frac{1}{f}(\Pi^+_I - \Pi^-_I)_{z'=-h_1}. \tag{3.23b}$$

Knowing p_g^+ one can determine p_g^- by continuity of pressure, $p_g^- = p_g^+|_{z=-h_1}$, and then η_g from (3.22*b*).

It is seen from (3.21) that the motion in the geostrophic mode occurs in planes parallel to the rigid boundaries, the motion in the homogeneous layer being columnar with columns elongated parallel to the angular rotation speed $\boldsymbol{\Omega}$. In the upper stratified layer the motion is more complicated; its structure is not columnar and depends on the initial horizontal velocity and density.

Under the TA (when $\alpha = 0$) the geostrophic mode is described by (3.21), (3.22) with x, y, z instead of x', y', z'. This means that the non-traditional terms are of importance in QG dynamics if the dominating horizontal scale L of initial perturbation is smaller than or of the order of the fluid depth:

$$L \leqslant H. \tag{3.24}$$

For a long-wave perturbation with

$$L \gg H \tag{3.25}$$

the contribution of the term αz in (3.13) is small, i.e. the non-traditional terms have a weak effect on the long-wave geostrophic mode.

The ageostrophic wave component $(\boldsymbol{u}_a, \rho_a, p_a)$ obeys the same equations (3.14*a–e*) but the invariants (3.16), (3.19) and the surface density $\rho_a(x', y', 0)$ are zero, i.e.

$$\Pi_a^+ = \partial_{x'} v_a^+ - \partial_{y'} u_a^+ - (fg/\rho_0)(\rho_a^+/N^2)_{z'} = 0, \tag{3.26a}$$

$$\Pi_a^- = \frac{1}{h_2}\int_{-H}^{-h_1} (\partial_{x'} v_a^- - \partial_{y'} u_a^-)\,\mathrm{d}z' - \frac{f}{h_2}\eta_a = 0, \tag{3.26b}$$

$$\rho_a^+|_{z'=0} = 0. \tag{3.26c}$$

The wave component is a superposition of harmonic waves considered in Reznik (2013). The waves are dispersive, therefore for localized initial conditions (when u_I, $v_I \to 0$ as $r = \sqrt{x^2 + y^2} \to \infty$) the wave part decays with increasing time at a fixed point in space and the full solution tends to the above stationary geostrophic mode. Thus, in the barotropic layer any localized initial state tends with time to a geostrophically balanced vortex state with axis parallel to $\boldsymbol{\Omega}$, exactly as in the purely barotropic case (Reznik 2014).

Nonlinear adjustment at small Rossby number $Ro = U/fL \ll 1$ (U is the horizontal velocity scale) results in a slow (as compared to the inertial time f^{-1}) evolution of the geostrophic component on the advective time $T_a = O(1/Rof)$. The scenario of the adjustment depends on the relationship between the typical flow velocity U and the group velocity c_g of the fast waves (see Reznik 2014 for more details). In the rest of paper we examine the nonlinear evolution of large-scale perturbations with $H \ll L \leqslant L_R$. It was shown in § 3.1 that in this range the wave spectrum consists of internal waves and the gyroscopic ones which are close to inertial oscillations. In view of (3.9) and (3.12) the corresponding group velocities c_g^{iw} and c_g^{gw} of the internal and gyroscopic waves are $O(fL_R)$ and $O(fH)$, respectively. For L in the range (3.4) and small Rossby number this means that the group velocity of internal waves greatly exceeds both the flow velocity U and the group velocity of gyroscopic waves, and the internal waves only weakly interact with the slow geostrophic component. At the same time, the interaction between the gyroscopic waves and geostrophic flow is much more effective, especially if $c_g^{gw} \leqslant U$. In what follows we assume that the group velocity c_g^{gw} is of the order of the flow velocity U:

$$c_g^{gw} = O(fH) \sim U. \tag{3.27}$$

4. Non-dimensional equations and asymptotic expansions

To write the system (2.2), (2.3), (2.4) in non-dimensional form we introduce the time scale $T=f^{-1}$, the vertical scale H, the horizontal scale $L=L_R$, the scales of horizontal and vertical velocities U and $W=(H/L)U$, respectively, and the scales of pressure $P=\rho_0 f LU$ and density variations $R=\rho_0 Ro(N_0^2H/g)$. The characteristic scale Z of the interface perturbation is obtained from (2.4*c*): $Z=RoH$.

In vector form the non-dimensional equations are written as:

$$\hat{\boldsymbol{u}}_t+Ro\,\hat{\boldsymbol{u}}\boldsymbol{\cdot}\hat{\boldsymbol{\nabla}}\hat{\boldsymbol{u}}+2\hat{\boldsymbol{\Omega}}\times\hat{\boldsymbol{u}}+\boldsymbol{e}_z\rho/\delta=-\hat{\boldsymbol{\nabla}}p, \tag{4.1a}$$

$$\rho_t+Ro\,\hat{\boldsymbol{u}}\boldsymbol{\cdot}\hat{\boldsymbol{\nabla}}\rho-N^2w=0,\quad \hat{\boldsymbol{\nabla}}\boldsymbol{\cdot}\hat{\boldsymbol{u}}=0 \tag{4.1b,c}$$

in the domain $0\geqslant z\geqslant -h_1+Ro\eta$; and

$$\hat{\boldsymbol{u}}_t+Ro\,\hat{\boldsymbol{u}}\boldsymbol{\cdot}\hat{\boldsymbol{\nabla}}\hat{\boldsymbol{u}}+2\hat{\boldsymbol{\Omega}}\times\hat{\boldsymbol{u}}=-\hat{\boldsymbol{\nabla}}p,\quad \hat{\boldsymbol{\nabla}}\boldsymbol{\cdot}\hat{\boldsymbol{u}}=0 \tag{4.2a,b}$$

in the domain $-h_1+Ro\eta\geqslant z\geqslant -1$. Here $\hat{\boldsymbol{u}}=(u,v,\delta w)$, $\hat{\boldsymbol{\nabla}}=(\partial_x,\partial_y,\partial_z/\delta)$, $2\hat{\boldsymbol{\Omega}}=\boldsymbol{e}_y\alpha+\boldsymbol{e}_z$, $\delta=H/L=f/N_0$; here and below the notation for non-dimensional h_1, h_2 and N remains unchanged. In the boundary and initial conditions (2.4), (2.7), (2.8) written in non-dimensional form the depth H is replaced by 1 and the interface surface becomes $z=-h_1+Ro\eta$.

We are interested in the case when the motion is large scale and the rotation is fast, i.e. both the aspect ratio δ and the Rossby number Ro are small parameters. The condition (3.27) means that

$$\delta=Ro. \tag{4.3}$$

The solution is represented in the following asymptotic form (e.g. Reznik, Zeitlin & Ben Jelloul 2001):

$$(u,v,w,p,\rho)=(u_0,v_0,w_0,p_0,\rho_0)(x,y,z,t,T_1,\ldots)+\delta(u_1,v_1,w_1,p_1,\rho_1)+\cdots \tag{4.4}$$

where $T_n=\delta^n t$, $n=1,2,\ldots$, are the slow times. Substitution of (4.4) into (4.1), (4.2) gives at the lowest order:

$$\partial_t u_0^\pm-v_0^\pm=-\partial_x p_0^\pm,\quad \partial_t v_0^\pm+u_0^\pm=-\partial_y p_0^\pm,\quad \rho_0^\pm=-\partial_z p_0^\pm, \tag{4.5a–c}$$

$$\partial_t\rho_0^\pm-N_\pm^2 w_0^\pm=0,\quad \partial_x u_0^\pm+\partial_y v_0^\pm+\partial_z w_0^\pm=0; \tag{4.5d,e}$$

$$w_0^+|_{z=0}=w_0^-|_{z=-1}=0, \tag{4.6a}$$

$$\lim_{z\to -h_1}\rho_0^+/N^2=\eta_0,\quad w_0^\pm|_{z=-h_1}=\partial_t\eta_0,\quad [u_0,v_0,p_0]=0, \tag{4.6b–d}$$

$$(u_0^\pm,v_0^\pm,\rho_0^\pm)_{t=0}=(u_I^\pm,v_I^\pm,\rho_I^\pm)(x,y,z). \tag{4.6e}$$

We note that the boundary condition (4.6*b*) is suitable both for the discontinuous profile $N(z)$ when $N(-h_1)\neq 0$ and the continuous one with $N(-h_1)=0$, and is consistent with (4.5*d*) and the boundary condition (4.6*c*).

At the first order we have:

$$\partial_t u_1^\pm-v_1^\pm=-\partial_{T_1}u_0^\pm-M_u^\pm-\alpha w_0^\pm-\partial_x p_1^\pm,\quad \partial_t v_1^\pm+u_1^\pm=-\partial_{T_1}v_0^\pm-M_v^\pm-\partial_y p_1^\pm, \tag{4.7a,b}$$

$$-\alpha u_0^\pm+\rho_1^\pm=-\partial_z p_1^\pm,\quad \partial_t\rho_1^\pm-N_\pm^2 w_1^\pm=-\partial_{T_1}\rho_0^\pm-M_\rho^\pm, \tag{4.7c,d}$$

$$\partial_x u_1^\pm+\partial_y v_1^\pm+\partial_z w_1^\pm=0. \tag{4.7e}$$

In (4.5)–(4.7) $\rho_0^-=\rho_1^-=N_-=0$, $N_+=N(z)$.

The first-order boundary and initial conditions are:

$$w_1^+|_{z=0} = w_1^-|_{z=-1} = 0; \tag{4.8a}$$

and at $z = -h_1$:

$$\rho_1^+ = N^2\eta_1 - \eta_0\partial_z\rho_0^+ + NN_z\eta_0^2, \quad [p_1] = -N^2\eta_0^2/2, \tag{4.8b,c}$$

$$w_1^\pm = \eta_{1t} - \eta_0\partial_z w_0^\pm + \partial_{T_1}\eta_0 + u_0^\pm\partial_x\eta_0 + v_0^\pm\partial_y\eta_0, \tag{4.8d}$$

$$[u_1] = -[\partial_z u_0]\eta_0, \quad [v_1] = -[\partial_z v_0]\eta_0, \tag{4.8e,f}$$

$$(u_1^\pm, v_1^\pm, \rho_1^\pm)_{t=0} = 0. \tag{4.8g}$$

Here $[a] = a^+|_{z=-h_1} - a^-|_{z=-h_1}$, N is the non-dimensional buoyancy frequency and

$$M_u^\pm = u_0^\pm\partial_x u_0^\pm + v_0^\pm\partial_y u_0^\pm + w_0^\pm\partial_z u_0^\pm, \tag{4.9a}$$

$$M_v^\pm = u_0^\pm\partial_x v_0^\pm + v_0^\pm\partial_y v_0^\pm + w_0^\pm\partial_z v_0^\pm, \tag{4.9b}$$

$$M_\rho^+ = u_0^+\partial_x\rho_0^+ + v_0^+\partial_y\rho_0^+ + w_0^+\partial_z\rho_0^+, \quad M_\rho^- = 0. \tag{4.9c,d}$$

5. The lowest-order solution

In this section the lowest-order problem (4.5) and (4.6) is examined. First we construct a solution of the initial problem not taking into account the dependence on slow times (the so-called standard solution). The standard solution is uniquely determined by the initial conditions (4.6*e*) and depends linearly on the initial fields u_I, v_I, ρ_I. To take into account the dependence on slow time, the initial fields in the standard solution are replaced by functions depending on the slow time; initial values of the functions are equal to u_I, v_I, ρ_I.

5.1. *Geostrophic component*

The system (4.5), up to constant coefficients, is a simplification of system (3.14) at $f_s = \alpha = 0$ and the analysis in § 3.2 is directly applied to (4.5). The invariants (3.16), (3.19) and (3.20) are now non-dimensional and take the form:

$$\Pi^+ = \partial_x v_0^+ - \partial_y u_0^+ - (\rho_0^+/N^2)_z = \Pi_I^+(x, y, z), \tag{5.1a}$$

$$\Pi^- = \frac{1}{h_2}\int_{-1}^{-h_1}(\partial_x v_0^- - \partial_y u_0^-)\mathrm{d}z - \frac{\eta_0}{h_2} = \Pi_I^-(x, y), \tag{5.1b}$$

$$\rho_0^+|_{z=0} = \rho_I^+(x, y, 0). \tag{5.1c}$$

Exactly as in § 3.2 the lowest-order solution is represented as the sum of a geostrophic part (coinciding with (3.21) *mutatis mutandis*) and an ageostrophic component with the zero invariants (5.1). For simplicity of notation the geostrophic and ageostrophic components will be denoted here by the subscripts 'g' and 'a' (without the subscript '0'). The QG potential vorticity in the layers (3.22) takes the form:

$$\Pi^+ = \nabla_h^2 p_g^+ + (\partial_z p_g^+/N^2)_z = \Pi_I^+(x, y, z), \tag{5.2a}$$

$$\Pi^- = \nabla_h^2 p_g^- - \eta_g/h_2 = \Pi_I^-(x, y). \tag{5.2b}$$

Equations (5.2) should be solved with the non-dimensional boundary conditions

$$\partial_z p_g^+|_{z=0} = -\rho_g^+|_{z=0} = -\rho_I^+(x, y, 0), \tag{5.3a}$$

$$\lim_{z\to -h_1}[(\partial_z p_g^+/N^2)_z - \partial_z p_g^+/(h_2 N^2)] = \Pi^+|_{z=-h_1} - \Pi^-, \tag{5.3b}$$

which follow from (3.23).

5.2. *Ageostrophic component*

The ageostrophic components in the layers obey (4.5), i.e.

$$\partial_t u_a^\pm - v_a^\pm = -\partial_x p_a^\pm, \quad \partial_t v_a^\pm + u_a^\pm = -\partial_y p_a^\pm, \quad \rho_a^\pm = -\partial_z p_a^\pm, \tag{5.4a–c}$$

$$\partial_t \rho_a^\pm - N_\pm^2 w_a^\pm = 0, \quad \partial_x u_a^\pm + \partial_y v_a^\pm + \partial_z w_a^\pm = 0, \quad \rho_a^- = 0. \tag{5.4d–f}$$

Boundary conditions for the ageostrophic quantities are the same as (4.6*a–d*) and the initial state is determined after calculating the geostrophic fields (see the previous subsection):

$$(u_a, v_a, \rho_a)_{t=0} = (u_{aI}, v_{aI}, \rho_{aI}) = (u_I - u_g, v_I - v_g, \rho_I - \rho_g). \tag{5.5}$$

In addition, the ageostrophic fields are imposed by the restrictions that the PV in the layers is zero:

$$\partial_x v_a^+ - \partial_y u_a^+ - (\rho_a^+/N^2)_z = 0, \quad \frac{1}{h_2}\int_{-1}^{-h_1} (\partial_x v_a^- - \partial_y u_a^-)\mathrm{d}z - \frac{\eta_a}{h_2} = 0, \tag{5.6a,b}$$

and the ageostrophic density at $z = 0$ is zero in view of (5.3*a*):

$$\rho_a^+|_{z=0} = 0. \tag{5.7}$$

5.2.1. *Some properties of the ageostrophic solution*

We now discuss some general properties of the ageostrophic component. One can show (see appendix B) that the vertically integrated ageostrophic horizontal velocities and pressure are zero:

$$\int_{-1}^{0} (u_a, v_a, p_a)\mathrm{d}z = 0. \tag{5.8}$$

The lower layer pressure p_a^- does not depend on z therefore:

$$p_a^- = -\frac{1}{h_2}\int_{-h_1}^{0} p_a^+ \mathrm{d}z. \tag{5.9}$$

Continuity of the pressure at the interface $z = -h_1$ gives the relation:

$$p_a^+|_{z=-h_1} + \frac{1}{h_2}\int_{-h_1}^{0} p_a^+ \mathrm{d}z = 0. \tag{5.10}$$

It readily follows from (5.4*a*,*b*) and (5.10) that

$$\partial_t \hat{u}_a^+ - \hat{v}_a^+ = 0, \quad \partial_t \hat{v}_a^+ + \hat{u}_a^+ = 0, \tag{5.11}$$

where

$$(\hat{u}_a^+, \hat{v}_a^+) = (u_a^+, v_a^+)|_{z=-h_1} + \frac{1}{h_2}\int_{-h_1}^{0} (u_a^+, v_a^+)\mathrm{d}z. \tag{5.12}$$

The solution to (5.11) is readily written:

$$\hat{u}_a^+ + \mathrm{i}\hat{v}_a^+ = (\hat{u}_{aI}^+ + \mathrm{i}\hat{v}_{aI}^+)\mathrm{e}^{-\mathrm{i}t}; \tag{5.13}$$

$\hat{u}_{aI}^+$, $\hat{v}_{aI}^+$ are the initial values of $\hat{u}_a^+$, $\hat{v}_a^+$.

An important point is that the upper stratified layer does not contain the inertial oscillations $\sim \sin t, \cos t$, i.e.

$$u_{as}^{+} = v_{as}^{+} = u_{ac}^{+} = v_{ac}^{+} = 0; \tag{5.14}$$

and similarly for other fields (see appendix C). Here

$$g_{s,c} = \lim_{T\to\infty} \frac{2}{T} \int_0^T (\sin t, \cos t) g(t) \mathrm{d}t. \tag{5.15}$$

In view of (5.14) the integral in (5.12) also does not contain the inertial oscillations, therefore, as readily follows from (5.12), (5.13), the horizontal velocities at the interface $(u_a^+, v_a^+)|_{z=-h_1}$ contain the inertial oscillations (5.13), i.e. (5.14) is valid for $z > -h_1$ and is not valid at $z = -h_1$. Such a solution structure is typical for a boundary layer (see also Reznik 2013) when at large times the velocity u_a^+ (for example) is represented in the form

$$u_a^+ = C_s[x, y, (z + h_1)t] \sin t + C_c[x, y, (z + h_1)t] \cos t \tag{5.16}$$

in a close vicinity of the interface $z = -h_1$. If the functions $C_{s,c}$ tend to zero as $t \to \infty$ at any fixed $z > -h_1$, but, for example, $C_s(x, y, 0) \neq 0$ then $u_{as}^+ = 0$ for $z > -h_1$ and $u_{as}^+ = C_s(x, y, 0) \neq 0$ at $z = -h_1$. We note that in the particular case of zero initial conditions for $\hat{u}_a^+, \hat{v}_a^+$ when

$$\hat{u}_{aI}^+ = \hat{v}_{aI}^+ = 0, \tag{5.17}$$

the relations (5.14) are valid everywhere in the upper layer $z \geqslant -h_1$ and the boundary layer in the vicinity of interface does not arise. We emphasize that details of the buoyancy frequency profile $N(z)$ are unimportant in the above consideration, therefore one can expect the boundary layer to exist for any upper layer stratification, i.e. for both smooth and discontinuous profiles of $N(z)$.

5.2.2. *Motion in the stratified upper layer*

In the upper layer equations (5.4*a–e*) can be reduced to one equation for the vertical velocity (e.g. Miropol'sky 2001):

$$(\partial_{tt} + 1)\partial_{zz} w_a^+ + N^2 \nabla_h^2 w_a^+ = 0, \tag{5.18}$$

which should be solved under the initial conditions:

$$(w_a^+, \partial_t w_a^+)_{t=0} = (w_I^+, \dot{w}_I^+)(x, y, z), \tag{5.19a}$$

the no-flux boundary condition:

$$w_a^+|_{z=0} = 0, \tag{5.19b}$$

and the boundary condition at $z = -h_1$ which simply follows from (5.12), (5.4*e*):

$$\left(\partial_z w_a^+ - \frac{1}{h_2} w_a^+\right)_{z=-h_1} = -(\partial_x \hat{u}_a^+ + \partial_y \hat{v}_a^+). \tag{5.19c}$$

In (5.19*a*) the function w_I^+ is equal to

$$w_I^+ = \int_z^0 D_I^+ \mathrm{d}z, \tag{5.20a}$$

and the function $\dot{w}_I^+$ is expressed in terms of the initial fields u_{aI}^+, v_{aI}^+, ρ_{aI}^+ (Reznik 2013):

$$\dot{w}_I^+ = \int_z^0 \zeta_{aI}^+ \mathrm{d}z + \int_z^0 \mathrm{d}z' \int_{-h_1}^{z'} \nabla_h^2 \rho_{aI}^+ \mathrm{d}z'' + z \int_{-h_1}^0 \mathrm{d}z \int_{-h_1}^z \nabla_h^2 \rho_{aI}^+ \mathrm{d}z'. \tag{5.20b}$$

In (5.20) and below the operators of two-dimensional divergence $D = u_x + v_y$ and vertical vorticity $\zeta = v_x - u_y$ are used; superscripts and subscripts on D, ζ denote the corresponding velocity fields.

Using (5.13), (5.11) one can represent (see appendix D for details) the boundary condition (5.19c) in the form:

$$\left(\partial_z w_a^+ - \frac{1}{h_2} w_a^+\right)_{z=-h_1} = \left[\left(\partial_z w_I^+ - \frac{1}{h_2} w_I^+\right)\cos t + \left(\partial_z \dot{w}_I^+ - \frac{1}{h_2}\dot{w}_I^+\right)\sin t\right]_{z=-h_1}. \tag{5.21}$$

The solution to (5.18), (5.19a,b), (5.21) is written as the sum

$$w_a^+ = w_u + w_I \cos t + \dot{w}_I \sin t, \tag{5.22}$$

where the auxiliary function w_u is a solution of the following forced problem with zero initial and boundary conditions:

$$(\partial_{tt} + 1)\partial_{zz} w_u + N^2 \nabla_h^2 w_u = -N^2 \nabla_h^2 [w_I^+ \cos t + \dot{w}_I^+ \sin t], \tag{5.23a}$$

$$w_u|_{z=0} = 0, \quad \left(\partial_z w_u - \frac{1}{h_2} w_u\right)_{z=-h_1} = 0, \tag{5.23b}$$

$$w_u|_{t=0} = \partial_t w_u|_{t=0} = 0. \tag{5.23c}$$

Now we represent all variables in (5.22), (5.23) in the form of Fourier integrals, for example

$$w_a^+ = \frac{1}{2\pi} \int \tilde{w}^+(k, l, z, t) \mathrm{e}^{\mathrm{i}(kx+ly)} \mathrm{d}k \mathrm{d}l; \tag{5.24}$$

and similarly for other values. Here and below the tilde denotes the Fourier amplitude of the corresponding variable. The amplitude $\tilde{w}_u = \tilde{w}_u(k, l, z, t)$ is sought as an expansion in the vertical modes which here are eigenfunctions of the problem:

$$W_{zz} + q^2 N^2 W = 0, \quad W|_{z=0} = 0, \quad \left(W_z - \frac{1}{h_2} W\right)_{z=-h_1} = 0. \tag{5.25}$$

The eigenfunctions W_n, eigenvalues q_n, and the corresponding wave frequencies σ_n are readily found in the case $N = \text{const.}$ (cf. (3.7)–(3.9)):

$$W_n = \sin q_n z, \quad q_n = s_n/h_1, \quad \sigma_n = \sqrt{1 + \kappa^2/q_n^2}, \quad n = 1, 2, \ldots; \tag{5.26}$$

here s_n is the nth root of (3.8).

The amplitude $\tilde{w}_u$ can be written as

$$\tilde{w}_u = \sum_{n=1}^{\infty} \left[\tilde{w}_{In}^+ \cos \sigma_n t + (\tilde{\dot{w}}_{In}^+/\sigma_n) \sin \sigma_n t\right] W_n - \tilde{w}_I^+ \cos t - \tilde{\dot{w}}_I^+ \sin t. \tag{5.27}$$

In view of (5.22), (5.27) the Fourier amplitude $\tilde{w}_a^+$ takes the form:

$$\tilde{w}_a^+ = \sum_{n=1}^{\infty} \left[\tilde{w}_{In}^+ \cos\sigma_n t + (\dot{\tilde{w}}_{In}^+/\sigma_n)\sin\sigma_n t \right] W_n(z). \tag{5.28}$$

We see that the upper layer ageostrophic component is the superposition of the long super-inertial internal waves $\sim \exp[\mathrm{i}(kx + ly - \sigma_n t)]$ considered in § 3. The function w_a^+ does not contain the inertial oscillations (see also § 5.2.1 above) and at the interface any finite partial sum of the series (5.28) satisfies the second boundary conditions (5.23*b*) instead of (5.21). This means that in the very close vicinity of the interface $z = -h_1$ the wave modes with very large values of n play an important role. Since $q_n \to \infty, \sigma_n \to 1$ for $n \to \infty$, vertical scales and frequencies of these modes are close to zero and to the inertial frequency, respectively. The joint effect of these modes forms the near-interface boundary layer considered below in § 5.2.4.

5.2.3. *Motion in the homogeneous lower layer*

It readily follows from (5.4*a,b,c,f*) that in the lower layer:

$$\partial_z(\partial_t u_a^- - v_a^-) = 0, \quad \partial_z(\partial_t v_a^- + u_a^-) = 0, \tag{5.29a,b}$$

whence

$$U_a^- = U_{aI}^-(x, y, z)\mathrm{e}^{-\mathrm{i}t} + \bar{U}(x, y, t). \tag{5.30}$$

Here $\bar{U} = \bar{u} + \mathrm{i}\bar{v}$ is still unknown depth-independent complex velocity and

$$U_a^- = u_a^- + \mathrm{i}v_a^-, \quad U_{aI}^- = u_{aI}^- + \mathrm{i}v_{aI}^-. \tag{5.31a,b}$$

Integrating (5.30) over z from -1 to $-h_1$ and using (5.8), (5.14) one finds:

$$\bar{U} = -\frac{\mathrm{e}^{-\mathrm{i}t}}{h_2}\int_{-1}^{-h_1} U_{aI}^- \mathrm{d}z + \bar{\bar{U}}(x, y, t), \tag{5.32}$$

$$\bar{\bar{U}}(x, y, t) = -\frac{1}{h_2}\int_{-h_1}^{0} U_a^+ \mathrm{d}z, \quad \bar{\bar{U}}_{s,c} = 0. \tag{5.33a,b}$$

The 'non-inertial' depth-independent velocity $\bar{\bar{U}}(x, y, t)$ is induced by the upper layer internal waves and can be calculated from the known vertical velocity w_a^+ which is given by (5.24), (5.28).

In view of (5.30), (5.32) the horizontal velocity U_a^- can be written as:

$$U_a^- = A(x, y, z)\mathrm{e}^{-\mathrm{i}t} + \bar{\bar{U}}(x, y, t), \tag{5.34}$$

$$A = A_I = U_{aI}^- - \frac{1}{h_2}\int_{-1}^{-h_1} U_{aI}^- \mathrm{d}z. \tag{5.35}$$

The velocity components are given by the formulae:

$$(u_a^-, v_a^-) = \left(\frac{1}{2}, \frac{-\mathrm{i}}{2}\right) A(x, y, z)\mathrm{e}^{-\mathrm{i}t} + \text{c.c.} + (\bar{\bar{u}}, \bar{\bar{v}})(x, y, t), \tag{5.36a}$$

$$w_a^- = -\frac{1}{2}\mathrm{e}^{-\mathrm{i}t}\int_{-1}^{z} s(A)\mathrm{d}z + \text{c.c.} - (z+1)(\bar{\bar{u}}_x + \bar{\bar{v}}_y), \quad s = \partial_x - \mathrm{i}\partial_y. \tag{5.36b}$$

It follows from (5.35) that

$$\int_{-1}^{-h_1} A\mathrm{d}z = 0. \tag{5.37}$$

Thus in the homogeneous layer the ageostrophic motion is the sum of inertial oscillations and a field induced by super-inertial internal waves. The condition (5.37) provides non-penetration of the inertial signal into the stratified layer in the vertical velocity field. If the amplitude of inertial oscillations A_I in (5.35) is zero at the interface $z=-h_1$:

$$A_I(x, y, -h_1) = 0, \tag{5.38}$$

then the non-penetration is provided for the horizontal velocity, too. One can readily show that (5.38) is equivalent to the condition (5.17) of absence of the boundary layer. Obviously, equation (5.38) and, therefore, (5.17) are fulfilled only for particular initial velocity fields; if this is not the case a non-stationary boundary layer develops near the interface.

5.2.4. *Boundary layer*

We now consider the case of general initial conditions when (5.38) is not valid and the inertial signal in the horizontal velocity is non-zero at the interface $z=-h_1$. As discussed above, in this case the solution in the domain $z \geqslant -h_1$ has a boundary layer structure in the vicinity of the interface at large times, and is described by formulae like (5.16). The representation (5.28), (5.24) of the solution as series in the eigenfunctions $W_n(z)$ is poorly suited to describing such regimes since any finite partial sum of the series (5.28) obeys the zero boundary conditions (5.23*b*) and, therefore, an infinite number of vertical modes with numbers $n \to \infty$ should be taken into account in the boundary layer domain.

To describe the boundary layer dynamics we introduce two new variables:

$$\bar{w}_s = \frac{1}{t}\int_0^t w_a^+ \sin t\mathrm{d}t, \quad \bar{w}_c = \frac{1}{t}\int_0^t w_a^+ \cos t\mathrm{d}t. \tag{5.39}$$

The meaning of the variables is that the impact of not near-inertial harmonics on $\bar{w}_{s,c}$ becomes negligible at large times $t \gg 1$ as seen from (5.28). We note that in a similar boundary layer problem for non-rotating SNS fluid (Reznik 2013) the different variable

$$\bar{w} = \frac{1}{t}\int_0^t w\mathrm{d}t \tag{5.40}$$

was used (see also Il'in 1970, 1972 and Kamenkovich & Kamenkovich 1993).

From (5.18), (5.19*b*), and (5.21) we find:

$$(t\bar{w})_{zztt} + 2\mathrm{i}(t\bar{w})_{zzt} + t\nabla_h^2\bar{w} = R = \partial_{zz}(-w_I^+ + \mathrm{i}\dot{w}_I^+), \quad \bar{w} = \bar{w}_s + \mathrm{i}\bar{w}_c; \tag{5.41a,b}$$

$$\bar{w}|_{z=0} = 0, \tag{5.42a}$$

$$\left(\bar{w}_z - \frac{1}{h_2}\bar{w}\right)_{z=-h_1} = \frac{1}{2}\left[\partial_z\dot{w}_I^+ - \frac{1}{h_2}\dot{w}_I^+ + \mathrm{i}\left(\partial_z w_I^+ - \frac{1}{h_2}w_I^+\right)\right]_{z=-h_1}. \tag{5.42b}$$

The boundary condition (5.42*b*) is written up to small terms of the order of $1/t$. When writing (5.41*a*) we assume for simplicity N to be constant, i.e. $N=1$.

Outside the boundary layers $\bar{w}_z \sim 1$, therefore an approximate solution $\bar{w}_0$ satisfying (5.41a) in this domain at large t is determined by the equation

$$t\nabla_h^2 \bar{w}_0 = R, \tag{5.43a}$$

i.e.

$$\bar{w}_0 = S(x, y, z)/t, \quad \nabla_h^2 S = R. \tag{5.43b,c}$$

One can readily check that the terms with derivatives with respect to z on the left-hand side of (5.41a), $(t\bar{w}_0)_{zztt}$ and $2\mathrm{i}(t\bar{w}_0)_{zzt}$, are much smaller than the term $t\nabla_h^2 \bar{w}_0$ and, therefore, are neglected when deriving (5.43).

Obviously, $\bar{w}_0$ satisfies neither (5.42a) (since, generally, $R|_{z=0} \neq 0$) nor (5.42b), therefore in the vicinities of the boundaries $z = 0, -h_1$ narrow boundary layers arise in which $\partial_z \gg 1$. In the boundary layer near interface the leading-order solution is sought in the form $\bar{w} = \bar{w}_b = t^{\alpha} \hat{w}_b(x, y, \xi)$ where $\xi = (z + h_1)t^{\beta}$ is the boundary layer stretched coordinate. The parameters α and β are determined from two conditions. First, as follows from the boundary condition (5.42b), $\partial_z \bar{w}_b = t^{\alpha+\beta} \partial_\xi \hat{w}_b \sim 1$, and, second, the maxima of the terms with derivatives with respect to z that were neglected outside the boundary layer, and the third term on the left-hand side of (5.41a) should be of the same order, i.e. $t^{2\beta-1} \sim 1$. As a result we have $\beta = -\alpha = 1/2$, i.e. in the boundary layer

$$\bar{w} = \bar{w}_b = \frac{1}{\sqrt{t}} \hat{w}_b(x, y, \xi), \quad \xi = (z + h_1)\sqrt{t} \tag{5.44}$$

(cf. Kamenkovich & Kamenkovich 1993; Reznik 2013). As seen from (5.44), for large t and $\xi = (z + h_1)\sqrt{t} \sim 1$ the boundary layer vertical velocity $\bar{w}$ tends to zero but the derivative $\bar{w}_z$ is of the order of unity.

Substituting (5.44) into (5.41a) and neglecting small terms we have:

$$\xi \partial_{\xi\xi\xi} \hat{w}_b + 3\partial_{\xi\xi} \hat{w}_b - \mathrm{i}\nabla_h^2 \hat{w}_b = 0. \tag{5.45}$$

Writing $\hat{w}$ in the form of the Fourier integral (5.24) one finds for the Fourier amplitude $\tilde{\hat{w}}_b$:

$$\xi \partial_{\xi\xi\xi} \tilde{\hat{w}}_b + 3\partial_{\xi\xi} \tilde{\hat{w}}_b + \mathrm{i}\kappa^2 \tilde{\hat{w}}_b = 0. \tag{5.46}$$

For the boundary layer to exist the solution $\tilde{\hat{w}}_0$ to (5.46) satisfying the conditions

$$\tilde{\hat{w}}_0 \to 0 \quad \text{as } \xi \to \infty; \quad \partial_\xi \tilde{\hat{w}}_0|_{\xi=0} = 1, \tag{5.47a,b}$$

must exist. Analysis in appendix E confirms the possibility of such a solution. The corresponding Fourier amplitude $\tilde{\bar{w}}$ is given by:

$$\tilde{\bar{w}}_b = \frac{1}{\sqrt{t}} C(k, l) \tilde{\hat{w}}_0(k, l, \xi), \quad C = \frac{1}{2}\left[\partial_z \tilde{\dot{w}}_I^+ - \frac{1}{h_2}\tilde{\dot{w}}_I^+ + \mathrm{i}\left(\partial_z \tilde{w}_I^+ - \frac{1}{h_2}\tilde{w}_I^+\right)\right]_{z=-h_1}. \tag{5.48a,b}$$

The boundary layer near the surface $z = 0$ is similar to that near the interface. From (5.18) and (5.19b) one obtains that

$$\partial_{zz} w_a^+|_{z=0} = \partial_{zz} \dot{w}_{aI}^+|_{z=0} \sin t + \partial_{zz} w_{aI}^+|_{z=0} \cos t, \tag{5.49}$$

i.e. at the surface the inertial signal arises in the vertical gradient of horizontal velocity (Maxim Kalashnik drew my attention to this fact). The near-surface boundary layer provides a 'buffer' zone between the surface and the internal domain where the inertial signal is prohibited. The leading-order boundary layer solution has the form:

$$\bar{w} = \bar{w}_s = \frac{1}{t}\hat{w}_s(x, y, \eta), \quad \eta = z\sqrt{t}. \tag{5.50}$$

Comparison of (5.44) and (5.50) shows that the near-surface boundary layer is weaker than the near-interface one. This is related to the fact that the interface inertial signal is stronger than the surface one: at the interface it emerges in the horizontal velocity itself and at the surface it is in the vertical gradient of the velocity. The equation for $\hat{w}_s$ is somewhat different from (5.45):

$$\eta\partial_{\eta\eta\eta}\hat{w}_s + 2\partial_{\eta\eta}\hat{w}_s - \mathrm{i}\nabla_h^2\hat{w}_s = -\mathrm{i}R|_{z=0}. \tag{5.51}$$

The solution $\hat{w}_s$ has the form (see (5.43)):

$$\hat{w}_s = S(x, y, 0) + \hat{w}_{s0}, \tag{5.52}$$

where $\hat{w}_{s0}$ obeys the homogeneous version of (5.51) and decays as $\eta \to \infty$. Analysis of the corresponding equation is very similar to that of (5.45) and demonstrates the existence of the required solution.

5.2.5. *Dependence on slow time*

The standard solution constructed above is the sum of a time-independent geostrophic component, lower layer inertial oscillations and dispersive internal waves; the non-stationary boundary layers are the result of joint impact of the internal waves with very short vertical lengths.

To derive the solution of the lowest-order system (4.5) and (4.6) depending on slow times one should 'allow' parameters related to the initial fields to depend on the slow times. The geostrophic part of the solution is determined by the PV $\Pi^{\pm}$ in the layers (see (5.2*a*) and (5.2*b*)) directly related to the initial fields u_I, v_I, ρ_I (see (5.1*a*) and (5.1*b*)). In what follows we assume that:

$$\Pi^{\pm} = \Pi^{\pm}(x, y, z, T_1, T_2, \ldots), \quad \Pi^{\pm}(x, y, z, 0, 0, \ldots) = \Pi_I^{\pm}. \tag{5.53a,b}$$

Similarly, for the internal waves the initial fields $(w_I^+, \dot{w}_I^+)(x, y, z)$ are replaced by the functions $(w_s^+, \dot{w}_s^+)(x, y, z, T_1, T_2, \ldots)$ with

$$(w_s^+, \dot{w}_s^+)(x, y, z, 0, 0, \ldots) = (w_I^+, \dot{w}_I^+)(x, y, z). \tag{5.54}$$

Finally, in the formulae (5.36), (5.37) describing the lower layer inertial oscillations we put:

$$A = A(x, y, z, T_1, T_2, \ldots), \quad A(x, y, z, 0, 0, \ldots) = A_I(x, y, z). \tag{5.55a,b}$$

The slow evolution of the fields (5.53)–(5.55) is determined from condition of boundedness of higher approximations. In the next section we analyse the first approximation to specify the dependence of the PV $\Pi^{\pm}$ and the amplitude A on the slow time T_1.

6. Slow evolution of the QG component and inertial oscillations

6.1. *Slow evolution of the QG component*

The slow evolution of the lowest-order QG component is determined from the first-order PV equations. Exclusion of the pressure from (4.7*a,b*) gives:

$$\partial_t \zeta_1^{\pm} + D_1^{\pm} = -\partial_{T_1}\zeta_0^{\pm} + \partial_y M_u^{\pm} - \partial_x M_v^{\pm} + \alpha \partial_y w_0^{\pm}. \tag{6.1}$$

In the upper layer the first-order PV equation is obtained using (6.1), (4.7*d,e*), and (5.1*a*):

$$\partial_t[\zeta_1^+ - \partial_z(\rho_1^+/N^2)] = -\Pi_{T_1}^+ + \partial_y M_u^+ - \partial_x M_v^+ + \partial_z(M_\rho^+/N^2) + \alpha \partial_y w_0^+. \tag{6.2}$$

To derive an analogous equation in the lower layer we integrate (6.1) over z from -1 to $-h_1$ and use (4.7*e*), (4.8*d*):

$$\begin{aligned}\left(\int_{-1}^{-h_1} \zeta_1^- \mathrm{d}z - \eta_1\right)_t &= -h_2\Pi_{T_1}^- + (u_0^-\partial_x\eta_0 + v_0^-\partial_y\eta_0 - \eta_0\partial_z w_0^-)_{z=-h_1} \\ &\quad + \int_{-1}^{-h_1} (\partial_y M_u^- - \partial_x M_v^- + \alpha\partial_y w_0^-)\mathrm{d}z. \end{aligned}\tag{6.3}$$

Now we average (6.2), (6.3) over the fast time t, i.e. apply the operation

$$\langle a \rangle = \lim_{T_a\to\infty} \frac{1}{T_a}\int_0^{T_a} a\mathrm{d}t; \tag{6.4}$$

as a result we have:

$$\Pi_{T_1}^+ = \langle \partial_y M_u^+ - \partial_x M_v^+ + (M_\rho^+/N^2)_z\rangle + \alpha\langle w_0^+\rangle_y, \tag{6.5}$$

$$\begin{aligned}\Pi_{T_1}^- &= \frac{1}{h_2}\langle u_0^-\partial_x\eta_0 + v_0^-\partial_y\eta_0 - \eta_0\partial_z w_0^-\rangle_{z=-h_1} \\ &\quad + \frac{1}{h_2}\int_{-1}^{-h_1}\langle \partial_y M_u^- - \partial_x M_v^- + \alpha\partial_y w_0^-\rangle \mathrm{d}z.\end{aligned}\tag{6.6}$$

When calculating the right-hand sides of (6.5), (6.6) we assume all fields to decay at infinity as $r = \sqrt{x^2+y^2} \to \infty$. The calculations are very similar to those in Reznik *et al.* (2001), Zeitlin, Reznik & Ben Jelloul (2003) and Reznik (2014) and are given in appendix F; here we present only the general ideas and results.

The zero-order solution in the upper layer is the sum of a slow QG flow and ageostrophic fast internal waves, therefore the nonlinear terms on the right-hand side of (6.5) contain slow–slow, slow–fast and fast–fast interactions. When averaging over the fast time (6.4) the contribution from slow–fast interaction vanishes since the time-averaged ageostrophic fields are zero. We assume the initial fields to be smooth; in this case the main part of the energy of the internal waves is accounted for by several first vertical modes; the energy of the boundary layer is negligible. Furthermore, all fields are horizontally localized and the energetically significant modes decay proportionally to $1/t$ at a fixed point x, y, z because of the horizontal dispersion (see (5.26) and Zeitlin *et al.* 2003). The boundary layer solutions also tend to zero at $t \to \infty$ and z fixed. Therefore, the contribution from self-interaction of the ageostrophic fields vanishes and (6.5) can be rewritten in the form of conservation of the upper layer quasi-geostrophic PV (see appendix F for details):

$$\Pi^+_{T_1} + J(p_g^+, \Pi^+) = 0, \tag{6.7a}$$

$$\Pi^+ = \Pi^+(x, y, z, T_1, \ldots) = \nabla_h^2 p_g^+ + (\partial_z p_g^+/N^2)_z. \tag{6.7b}$$

In (6.6) the contribution from the induced internal waves also vanishes but that from the inertial oscillations can be non-zero since the lowest-order inertial oscillations in (5.34) are non-propagating on times $t \ll 1/\delta$ and their self-interaction, in principle, can give rise to terms which do not depend on the fast time t. However, detail calculations (see appendix F) show that similarly to the barotropic case (Reznik 2014) these terms cancel each other and the resulting PV-equation in the lower layer can be written as

$$\Pi^-_{T_1} + J(p_g^-, \Pi^-) = 0, \quad \Pi^- = \Pi^-(x, y, T_1, \ldots) = \nabla_h^2 p_g^- - \eta_g/h_2. \tag{6.8a,b}$$

The QG lower layer pressure p_g^- is related to p_g^+ by the continuity at the interface:

$$p_g^- = p_g^+|_{z=-h_1}. \tag{6.9}$$

The boundary condition (5.3a) for p_g^+ at $z=0$ can be used only to calculate the initial geostrophic pressure; on times $t \sim 1/\delta$ one should take into account the slow evolution of density which is unknown in advance. To derive the boundary condition we consider (4.7d) at $z=0$:

$$\partial_t \rho_1^+ = -\partial_{T_1}\rho_0^+ - u_0^+ \partial_x \rho_0^+ - v_0^+ \partial_y \rho_0^+. \tag{6.10}$$

Applying the time averaging (6.4)–(6.10) and expressing the density ρ_g^+ in terms of the pressure p_g^+ one obtains the boundary condition for p_g^+:

$$\partial_{zT_1} p_g^+ + J(p_g^+, \partial_z p_g^+) = 0 \quad \text{at } z=0. \tag{6.11}$$

6.2. *Slow evolution of the inertial oscillations*

In this subsection all quantities are related to the lower layer; the superscript '−' is omitted for brevity. To derive equations for the first-order inertial oscillations we average (4.7a,b) over the lower layer depth and subtract the resulting equations from (4.7a,b); as a result we have:

$$\partial_t \tilde{u}_1 - \tilde{v}_1 = -\partial_{T_1}\tilde{u}_a - \tilde{M}_u - \alpha\tilde{w}_0 - \partial_x \tilde{p}_1, \tag{6.12a}$$

$$\partial_t \tilde{v}_1 + \tilde{u}_1 = -\partial_{T_1}\tilde{v}_a - \tilde{M}_v - \partial_y \tilde{p}_1. \tag{6.12b}$$

Here

$$(\tilde{u}_1, \tilde{v}_1, \ldots) = (u_1 - \langle u_1\rangle^z, v_1 - \langle v_1\rangle^z, \ldots), \quad \langle a\rangle^z = \frac{1}{h_2}\int_{-1}^{-h_1} a\,\mathrm{d}z, \tag{6.13}$$

and (see (5.34), (5.37)):

$$\tilde{U}_a = \tilde{u}_a + \mathrm{i}\tilde{v}_a = A(x, y, z, T_1, \ldots)\mathrm{e}^{-\mathrm{i}t}. \tag{6.14}$$

Rewriting (6.12) in the complex form

$$\partial_t \tilde{U}_1 + \tilde{U}_1 = -\partial_{T_1} \tilde{U}_a - (\partial_x \tilde{p}_1 + \mathrm{i}\partial_y \tilde{p}_1) - (\tilde{M}_u + \mathrm{i}\tilde{M}_v) - \alpha \tilde{w}_0, \tag{6.15}$$

where $\tilde{U}_1 = \tilde{u}_1 + \mathrm{i}\tilde{v}_1$, one concludes that the bounded solution $\tilde{U}_1$ exists if the right-hand side of (6.15) does not contain resonance terms $\sim \mathrm{e}^{-\mathrm{i}t}$. Analysis of the terms in (6.15) is very similar to the corresponding analysis in the barotropic case in Reznik (2014) and gives that the right-hand side of (6.15) is non-resonant under the condition (see appendix G for details):

$$A_{T_1} + J(p_g^-, A) + \frac{\mathrm{i}}{2}\nabla_h^2 p_g^- A + \mathrm{i}\alpha \left(\int_{-1}^{z} A \mathrm{d}z + \frac{1}{h_2} \int_{-1}^{-h_1} z A \mathrm{d}z \right)_y = 0. \tag{6.16}$$

In addition to (6.16) the amplitude A should satisfy the condition (5.37) which prevents the inertial signal in the vertical velocity from penetrating into the stratified upper layer.

6.3. *Discussion of the slow evolution*

The complete set of equations describing the slow evolution of the QG component on times $t \sim 1/\delta$ includes two PV-equations (6.7), (6.8), the boundary conditions (6.11), (5.3*b*) and the initial conditions (5.53*b*). The algorithm for calculation of the QG component is as follows. Knowing $p_g^+(T_1)$ one determines from (6.7*b*), (6.8*b*) the PVs $\Pi^+(T_1)$, $\Pi^-(T_1)$, then from (6.7*a*), (6.8*a*), (6.11) the fields $\Pi^+(T_1 + \Delta T)$, $\Pi^-(T_1 + \Delta T)$, $\partial_z p_g^+(T_1 + \Delta T)|_{z=0}$, respectively. Knowing the PVs Π^+, Π^- at the step $T_1 + \Delta T$ one can calculate the right-hand side in the boundary condition (5.3*b*), and determine the field $p_g^+(T_1 + \Delta T)$ from (6.7*b*) and the 'new' boundary conditions for p_g^+ at $z = 0, -h_1$.

The QG component conserves its energy; it can be derived from (6.7), (6.8), (A 3), (A 6) and (6.11) that:

$$E = E^+ + E^- = \text{const.}, \tag{6.17a}$$

$$E^+ = \frac{1}{2}\int \mathrm{d}x\mathrm{d}y \int_{-h_1}^{0} \mathrm{d}z \left[(\nabla_h p_g^+)^2 + \frac{(\partial_z p_g^+)^2}{N^2} \right], \quad E^- = \frac{h_2}{2}\int \mathrm{d}x\mathrm{d}y (\nabla_h p_g^-)^2. \tag{6.17b,c}$$

Here E is the full QG energy, E^+ and E^- are the energies of the upper and lower layers, respectively.

Let the QG motion in the lower layer be absent at some time $T_1 = T_I$, i.e.

$$p_g^- = p_g^+|_{z=-h_1} = 0. \tag{6.18}$$

Generally, for times $T_1 > T_I$ the QG pressure p_g^- becomes non-zero, i.e. the QG energy transfers into the lower layer. To show this we assume that (6.18) is fulfilled at all times. In this case the quantities $\Pi^+|_{z=-h_1}$, Π^- do not depend on time by virtue of (6.7*a*), (6.8*a*), and we have from (5.2*a*) an additional boundary condition for p_g^+ at $z = -h_1$:

$$\lim_{z \to -h_1} (\partial_z p_g^+ / N^2)_z = \Pi_I^+|_{z=-h_1}. \tag{6.19}$$

Obviously, the problem (6.7), (6.18), (6.19), (5.3*b*) and (6.11) is overdetermined and hence (6.18) cannot be valid for all times.

Equation (6.16) for the amplitude of inertial oscillations almost exactly coincides with the corresponding equation for the barotropic case (equation (6.17) in Reznik 2014). The last term in (6.16) arises due to the non-zero horizontal component of the Earth's rotation. Under the TA $\alpha = 0$ and the inertial oscillations are trapped by the QG component. The 'non-traditional' term results in a meridional dispersion of the inertial oscillations and in doing so it provides an effective energy radiation from the initial perturbation domain (see Reznik 2014 for more details).

Similarly to the barotropic case the slow QG component does not depend on the fast ageostrophic waves on times $\sim 1/\delta$, whereas evolution of the inertial oscillations depends on the geostrophic streamfunction p_g^-. At the same time, it follows from (6.16) and (5.37) that

$$\frac{\partial}{\partial T_1} \int \mathrm{d}x\mathrm{d}y \int_{-1}^{-h_1} \mathrm{d}z |A|^2 = 0, \tag{6.20}$$

i.e. the total energy of inertial oscillations is conserved along with that of the QG component. We note, however, that the conservation takes place on times $\sim 1/\delta$; on longer times the 'non-traditional' terms in the equations of motion can, in principle, give rise to energy exchange between the components as takes place for the barotropic fluid (Reznik 2014). If this is the case, the energy of QG motion in the lower layer can be transferred to the inertial oscillations. Of course, the mechanism of dissipation of QG energy in a homogeneous layer is highly speculative and it would be useful to verify it numerically using a non-hydrostatic model without the TA.

It was shown in § 5 that the condition (5.37) prevents the inertial signal in the vertical velocity field from penetrating into the stratified layer. Equation (6.16) 'supports' the limitation (5.37): it is readily to show by integrating (6.16) over z from -1 to $-h_1$ that if (5.37) is fulfilled at some moment T_0 then it is valid for all times $T > T_0$. If the initial conditions do not satisfy (5.17) and, therefore, equation (5.38), then the analogous screening in horizontal velocity is provided by a non-stationary boundary layer developing in the upper layer near the interface. Generally, the condition (5.38) is not supported by (6.16) because of the 'non-traditional' term in (6.16), i.e. the quantity $A|_{z=-h_1}$ ceases to be zero even if (5.38) is fulfilled at some moment. This means that without the TA the near-interface boundary layer develops for any initial conditions.

7. Summary and conclusions

We have examined nonlinear geostrophic adjustment in SNS fluid consisting of a stratified upper layer with $N \gg f$ and a homogeneous lower layer, the density and other fields being continuous at the interface between the layers. The traditional and hydrostatic approximations are not used. The wave spectrum in the model consists of internal and gyroscopic waves. The theory is developed for perturbations with typical horizontal scale L of the order of the Rossby scale L_R; in this case the internal waves are strongly dispersive and penetrate into the homogeneous lower layer down to the bottom. On the other hand, the gyroscopic waves are close to weakly dispersive inertial oscillations confined to the lower layer.

The general scenario of the geostrophic adjustment is a standard one (cf. Reznik *et al.* 2001; Zeitlin *et al.* 2003; Reznik 2014): an arbitrary perturbation is split in a unique way into slow and fast components evolving with characteristic time scales $(Ro f)^{-1}$ and f^{-1}, respectively. The slow component is close to the geostrophic balance and, in the case considered, is governed by two coupled nonlinear equations of conservation of QG potential vorticity in the upper and lower layers. The upper layer PV is the same as that in continuously stratified fluid; in the lower layer the QG motion does not depend on depth and the PV here is a sum of QG relative vorticity and the vortex-tube stretching due to variations in the interface height. The upper and lower layer QG flows are not independent: if at some moment the QG motion in the lower layer vanishes then at subsequent times the QG energy is transferred from the upper layer to the lower one. On times $t \sim (f\,Ro)^{-1}$ the slow component is not influenced by the fast one.

The fast component is a sum of the internal waves and the inertial oscillations confined to the lower layer and modulated by an amplitude depending on coordinates and the slow time. The inertial oscillations are long gyroscopic waves; depth-integrated horizontal flow induced by the oscillations is zero. On times $t \sim (f\,Ro)^{-1}$ the energy of inertial oscillations is conserved but they are coupled to the slow component: their amplitude obeys an equation that practically coincides with that in the barotropic case (Reznik 2014). Under the TA the inertial oscillations are trapped by the QG component; dispersion of the inertial oscillations packet occurs on times $t \sim (f\,Ro^2)^{-1}$. Without the TA the 'non-traditional' terms in the amplitude equation result in a meridional dispersion of the inertial oscillations on much shorter times $t \sim (f\,Ro)^{-1}$ and in doing so the terms provide an effective energy radiation from the initial perturbation domain.

Another feasible effect of the 'non-traditional' terms is an energy exchange between the slow QG component and inertial oscillations in the homogeneous layer on times $O(f^{-1}Ro^{-2})$. The possibility of such an exchange in the barotropic case was demonstrated by Reznik (2014). In the case of SNS fluid one can speculate that the QG energy is transferred from the stratified layer to the homogeneous one and then to the fast inertial oscillations. It would be useful to elucidate the existence and efficiency of this mechanism using a non-hydrostatic numerical model without the TA.

Inertial oscillations with horizontal scale $L \leqslant L_R$ cannot exist in the stratified upper layer. To prevent their penetration from the lower layer to the upper one, a non-stationary boundary layer develops in the upper layer near the interface at large times. The boundary layer is a result of joint impact of internal modes with large vertical wavenumbers whose frequencies are close to the inertial frequency f. Thus the near-interface domain is characterized by large vertical gradients of the horizontal velocities that can result in strong mixing and instability there. A similar boundary layer with weaker vertical gradients forms near the upper boundary at which the inertial signal emerges in the vertical gradients of horizontal velocities. Another mechanism of deep ocean mixing related to the horizontal component of the Earth's rotation and the beta-effect was suggested by Shrira & Townsend (2010, 2013).

The boundary layers in this and other works (Il'in 1970, 1972; Kamenkovich & Kamenkovich 1993; Reznik 2013) arise due to the existence of a limit point in the frequency spectrum when the wave frequency tends to a finite limit as the wavenumber tends to infinity. In the cited works the limit frequency is zero and the wavenumber in the case of Rossby waves is the horizontal wavenumber, while in the case of non-rotating SNS fluid it is the vertical one. In our case the limit frequency is the inertial frequency and the wavenumber is vertical (the horizontal wavenumber is fixed). The key point is that the phase and group speeds of waves with large wavenumbers have opposite signs (probably, this is a typical situation when the limit point exists). Therefore, one can say that the boundary oscillating with the limit frequency acts as a source of very short waves with phase speeds directed out of the boundary and group speeds directed towards the boundary. Such wavepackets cannot move far from the boundary and form the boundary layer with increasing time.

If initial fields decay at infinity in the horizontal plane then the energy-containing part of the internal waves decays at a fixed point with increasing time because of dispersion. The residual motion consists of the slow QG component and the inertial oscillations confined to the lower layer. We recall that in geostrophic adjustment with gravity waves (surface or internal) the inertial oscillations arise only if the dominating scale L of the initial perturbation exceeds the corresponding Rossby scale L_R, i.e. $L \gg L_R$ (cf. Reznik *et al.* 2001; Zeitlin *et al.* 2003). The slow QG component in this case obeys the so-called frontal dynamics equation. In the presence of gyroscopic waves the 'shorter' inertial oscillations with scales $H \ll L \leqslant L_R$ are possible. The significant vertical velocities of the near-inertial oscillations observed by van Haren & Millot (2005) in the practically barotropic deep Western Mediterranean Sea can be related to this property of gyroscopic waves.

A natural extension of the model considered is a fluid with a weakly stratified lower layer with non-zero buoyancy frequency N_- smaller than or of the order of f. This problem is more complicated because it lacks a simple solution in the lower layer. However, analysis shows that the wave solutions (3.3) for the vertical velocity are qualitatively similar to those in the SNS fluid. The modes with moderate vertical wavenumbers $n \ll N_+/f$ oscillate 'smoothly' in the upper strongly stratified layer and are approximately linear in z in the lower one. For $L \sim L_R$ these waves are strongly dispersive. At the same time, the modes with large wavenumbers $n \sim N_+/f$ are confined mainly to the lower layer: they oscillate 'smoothly' in the lower layer and 'rapidly' in the upper one, the amplitude of the oscillations in the upper layer being much less than in the lower one. For $L \sim L_R$ these modes are close to weakly dispersive (in the horizontal plane) inertial oscillations as in the SNS fluid. Thus one can assume that the long-term evolution of the vertical velocity is qualitatively similar to that in the SNS fluid: with time the modes with moderate numbers n decay because of dispersion and the vertical velocity becomes confined mainly to the lower layer. The behaviour of the horizontal velocity and boundary layer near the interface is more complicated and needs a special examination which will be done elsewhere.

Acknowledgements

The author thanks S. Badulin, E. Benilov, M. Kalashnik and V. Shrira for helpful comments and discussions. This work was supported by the RFBR grants 14-05-00070, 13-05-00463.

Appendix A. Linearized boundary conditions at $z' = -h_1$

It follows from (2.4*b*) that for small deviations η:

$$\rho|_{z=-h_1+\eta} = -\partial_z \rho_s(-h_1)\eta - \tfrac{1}{2}\partial_{zz}\rho_s(-h_1)\eta^2 + O(\eta^3); \tag{A 1}$$

therefore the boundary condition at the interface $z' = -h_1$ depends on the profile of the buoyancy frequency $N^2 = -g\partial_z\rho_s/\rho_0$. If $N(z)$ is discontinuous, i.e. $\partial_z\rho_s(-h_1) \neq 0$, then linearization of (A 1) gives

$$\rho/N^2|_{z=-h_1} = \rho_0\eta/g. \tag{A 2}$$

Using (3.21*d*) and (A 2), one can express the geostrophic deviation of the interface η_g in terms of the pressure p_g^+:

$$\eta_g = -(\partial_{z'} p_g^+/N^2)|_{z'=-h_1}. \tag{A 3}$$

From (A 3), (3.22) and the geostrophic pressure continuity $[p_g]=0$ one obtains the following boundary condition for (3.22*a*):

$$\left[(\partial_{z'}p_g^+/N^2)_{z'} - \partial_{z'}p_g^+/(h_2N^2)\right]_{z'=-h_1} = \frac{1}{f}(\Pi_I^+ - \Pi_I^-)_{z'=-h_1}. \tag{A 4}$$

If, however, $N(z)$ is smooth, i.e. $\partial_z\rho_s(-h_1)=0$, then the linearized condition (A 1) is written as

$$\rho|_{z=-h_1} = 0. \tag{A 5}$$

The behaviour of the density ρ near $z=-h_1$ should be consistent with (A 5), the linearized density equation (2.2*b*) $\rho_t - \rho_0 N^2 w/g = 0$, the kinematic condition (2.4*c*) $w|_{z=-h_1} = \eta_t$, and with the condition (A 2) valid for any non-zero $N(-h_1)$. One can readily see that the condition

$$\lim_{z\to -h_1} \rho/N^2 = \rho_0\eta/g \tag{A 6}$$

complies with the requirements. The condition (A 4) is rewritten in this case as

$$\lim_{z'\to -h_1} \left[(\partial_{z'}p_g^+/N^2)_{z'} - \partial_{z'}p_g^+/(h_2N^2)\right] = \frac{1}{f}(\Pi_I^+ - \Pi_I^-)_{z'=-h_1}. \tag{A 7}$$

Obviously, the condition (A 7) is suitable both for the discontinuous and continuous $N(z)$ profiles.

Appendix B. Some properties of the ageostrophic solution

The continuity of w_0 at $z=-h_1$ requires that in view of the continuity equations (5.4*e*)

$$\int_{-h_1}^{0} D_a^+ \mathrm{d}z + \int_{-1}^{-h_1} D_a^- \mathrm{d}z = 0; \quad D_a^\pm = \partial_x u_a^\pm + \partial_y v_a^\pm. \tag{B 1a,b}$$

Using (5.6*a,b*), (5.7), and (4.6*b*) written for the ageostrophic values one obtains:

$$\int_{-h_1}^{0} \zeta_a^+ \mathrm{d}z + \int_{-1}^{-h_1} \zeta_a^- \mathrm{d}z = 0; \quad \zeta_a^\pm = \partial_x v_a^\pm - \partial_y u_a^\pm. \tag{B 2a,b}$$

In view of (5.4*a,b*) we have

$$\partial_t D_a^\pm - \zeta_a^\pm = -\nabla_h^2 p_a^\pm, \tag{B 3}$$

whence taking into account (B 1), (B 2) one obtains

$$\nabla_h^2\left(\int_{-h_1}^{0} p_a^+ \mathrm{d}z + \int_{-1}^{-h_1} p_a^- \mathrm{d}z\right) = 0. \tag{B 4}$$

We assume all the fields to decay at infinity; in this case it follows from (B 1), (B 2), and (B 4) that the vertically integrated ageostrophic horizontal velocities and pressure are zero, i.e.

$$\int_{-h_1}^{0} (u_a^+, v_a^+, p_a^+)\mathrm{d}z + \int_{-1}^{-h_1} (u_a^-, v_a^-, p_a^-)\mathrm{d}z = 0. \tag{B 5}$$

Appendix C. Absence of inertial signal in the upper layer fields

We apply the operation (5.15) to (5.4) with superscript '+'; as a result we have (subscript 'a' is omitted for brevity):

$$u_c^+ + v_s^+ = \partial_x p_s^+, \quad v_c^+ - u_s^+ = \partial_y p_s^+, \quad \rho_s^+ = -\partial_z p_s^+, \tag{C 1a–c}$$

$$\rho_c^+ + N^2 w_s^+ = 0, \quad u_{sx}^+ + v_{sy}^+ + w_{sz}^+ = 0; \tag{C 1d,e}$$

$$u_s^+ - v_c^+ = -\partial_x p_c^+, \quad v_s^+ + u_c^+ = -\partial_y p_c^+, \quad \rho_c^+ = -\partial_z p_c^+, \tag{C 2a–c}$$

$$\rho_s^+ - N^2 w_c^+ = 0, \quad u_{cx}^+ + v_{cy}^+ + w_{cz}^+ = 0. \tag{C 2d,e}$$

Also one obtains from (5.6a):

$$\partial_x v_s^+ - \partial_y u_s^+ - (\rho_s^+/N^2)_z = 0, \quad \partial_x v_c^+ - \partial_y u_c^+ - (\rho_c^+/N^2)_z = 0. \tag{C 3a,b}$$

Using (C 1a,b,d,e), (C 2a,b,d,e), (C 3) and decay at infinity one finds:

$$\nabla_h^2 p_{s,c}^+ = 0 \Rightarrow p_{s,c}^+ = 0 \Rightarrow \rho_{s,c}^+ = w_{s,c}^+ = 0. \tag{C 4a–c}$$

Finally, from (C 1e), (C 2e), (C 3), and (C 4c) we have:

$$\nabla_h^2 u_{s,c}^+ = \nabla_h^2 v_{s,c}^+ = 0, \tag{C 5}$$

whence (5.14) follows.

Appendix D. Derivation of the boundary condition (5.21)

Taking (5.13) into account the right-hand side of (5.19c) can be written as:

$$\partial_x \hat{u}_a^+ + \partial_y \hat{v}_a^+ = \hat{D}_{aI}^+ \cos t + \hat{\zeta}_{aI}^+ \sin t, \tag{D 1}$$

where $\hat{D}_{aI}^+ = \partial_x \hat{u}_{aI}^+ + \partial_y \hat{v}_{aI}^+$, $\hat{\zeta}_{aI}^+ = \partial_x \hat{v}_{aI}^+ - \partial_y \hat{u}_{aI}^+$. Using (5.12), (5.4$e$) one finds that

$$\hat{D}_a^+ = \partial_x \hat{u}_a^+ + \partial_y \hat{v}_a^+ = -\left(\partial_z w_a^+ - \frac{1}{h_2} w_a^+\right)_{z=-h_1}, \tag{D 2}$$

$$\hat{\zeta}_a^+ = \partial_x \hat{v}_a^+ - \partial_y \hat{u}_a^+ = \partial_t \hat{D}_a^+ = -\left(\partial_z \dot{w}_a^+ - \frac{1}{h_2} \dot{w}_a^+\right)_{z=-h_1}, \tag{D 3}$$

therefore the condition (5.19c) is represented in the form (5.21):

$$\left(\partial_z w_a^+ - \frac{1}{h_2} w_a^+\right)_{z=-h_1} = \left(\partial_z w_I^+ - \frac{1}{h_2} w_I^+\right)_{z=-h_1} \cos t + \left(\partial_z \dot{w}_I^+ - \frac{1}{h_2} \dot{w}_I^+\right)_{z=-h_1} \sin t. \tag{D 4}$$

Appendix E. Boundary layer equation

Equation (5.46) has a weak singular point $\xi = 0$ and a strong singular point $\xi = \infty$ (Kamke 1976). In the vicinity of $\xi = 0$ two of three linearly independent solutions of (5.46) are regular, i.e. for example

$$\tilde{\tilde{w}}_1 = \sum_{n=0}^{\infty} a_n^{(1)} \xi^n, \quad \tilde{\tilde{w}}_2 = \sum_{n=0}^{\infty} a_n^{(2)} \xi^n, \tag{E 1a,b}$$

and the third one is singular:

$$\tilde{\tilde{w}}_3 = \ln \xi \sum_{n=0}^{\infty} a_{2n}^{(3)} \xi^{2n+1} + \xi^{-1} \sum_{n=0}^{\infty} b_{2n}^{(3)} \xi^{2n}. \tag{E 1c}$$

Here $a_n^{(1,2)}$, $a_{2n}^{(3)}$, $b_{2n}^{(3)}$ are constant coefficients; $2a_0^{(3)} + \mathrm{i}\kappa^2 b_0^{(3)} = 0$.

To find asymptotics at infinity a new variable g is introduced:

$$\tilde{\tilde{w}} = \xi^{-1/3} g(\xi^{2/3}). \tag{E 2}$$

The corresponding equation for g has the form:

$$g_{\mu\mu\mu} + \tfrac{3}{2}\mu^{-1} g_{\mu\mu} - 2\mu^{-2} g_\mu + \left(\tfrac{27}{8}\mathrm{i}\kappa^2 + \mu^{-3}\right) g = 0, \quad \mu = \xi^{2/3}. \tag{E 3}$$

Of the three linearly independent solutions to (E 3), for large μ the first one exponentially grows, the second one is a harmonic function, and the third one exponentially decays:

$$g_1 = \mathrm{e}^{\gamma\mu}(\cos\beta\mu - \mathrm{i}\sin\beta\mu + O(1/\mu)), \tag{E 4a}$$

$$g_2 = \cos 2\beta\mu + \mathrm{i}\sin 2\beta\mu + O(1/\mu), \tag{E 4b}$$

$$g_3 = \mathrm{e}^{-\gamma\mu}(\cos\beta\mu - \mathrm{i}\sin\beta\mu + O(1/\mu)); \tag{E 4c}$$

here $\gamma = 3\sqrt{3}\kappa^{2/3}/4$, $\beta = 3\kappa^{2/3}/4$. Obviously the solutions $\tilde{\tilde{w}}$ corresponding to g_2, g_3 decay at $\xi \to \infty$.

Solutions $\tilde{\tilde{w}}_1$, $\tilde{\tilde{w}}_2$ that are linearly independent and regular at $\xi = 0$ have linearly independent asymptotics as $\xi \to \infty$:

$$\tilde{\tilde{w}}_i = a_1^{(i)} \xi^{-1/3} g_1 + a_2^{(i)} \xi^{-1/3} g_2 + a_3^{(i)} \xi^{-1/3} g_3, \quad i = 1, 2, \tag{E 5}$$

whence it follows that the function

$$\tilde{\tilde{w}}_0 = a_1^{(2)} \tilde{\tilde{w}}_1 - a_1^{(1)} \tilde{\tilde{w}}_2 \tag{E 6}$$

is the non-trivial solution to (5.46) regular at $\xi = 0$ and decaying as $\xi \to \infty$.

Appendix F. Some details of derivation of PV equations

In view of (4.9) the first term on the right-hand side of (6.5) can be rewritten as:

$$\begin{aligned}\langle \partial_y M_u^+ - \partial_x M_v^+ + (M_\rho^+/N^2)_z \rangle = & -\langle u_0^+ \Pi_x^+ + v_0^+ \Pi_y^+ \rangle + \langle \partial_z u_0^+ \partial_x \rho_0^+ + \partial_z v_0^+ \partial_y \rho_0^+ \rangle / N^2 \\ & + \langle \partial_z w_0^+ \zeta_0^+ - w_0^+ \partial_z \zeta_0^+ + \partial_y w_0^+ \partial_z u_0^+ \\ & - \partial_x w_0^+ \partial_z v_0^+ + [(w_0^+ \partial_z \rho_0^+)/N^2]_z \rangle.\end{aligned} \tag{F 1}$$

Taking into account the geostrophic relations (3.21*a*–*d*) and the fact that the fast–slow and fast–fast interactions vanish under the averaging (6.4) one arrives at (6.7*a*).

One finds that in (6.6):

$$M_u^- = u_g^- \partial_x u_0^- + v_g^- \partial_y u_0^- + M_u^{(a)}, \quad M_v^- = u_g^- \partial_x v_0^- + v_g^- \partial_y v_0^- + M_v^{(a)}; \tag{F 2a,b}$$

$$M_u^{(a)} = u_a^- \partial_x u_0^- + v_a^- \partial_y u_0^- + w_0^- \partial_z u_0^-, \tag{F 3a}$$
$$M_v^{(a)} = u_a^- \partial_x v_0^- + v_a^- \partial_y v_0^- + w_0^- \partial_z v_0^-, \tag{F 3b}$$

whence it follows that

$$\begin{aligned}\langle \partial_y M_u^- - \partial_x M_v^- \rangle^z = {} & -u_g^- \langle \zeta_0^- \rangle_x^z - v_g^- \langle \zeta_0^- \rangle_y^z + \partial_y u_g^- \langle u_a^- \rangle_x^z + \partial_y v_g^- \langle u_a^- \rangle_y^z - \partial_x u_g^- \langle v_a^- \rangle_x^z \\ & - \partial_x v_g^- \langle v_a^- \rangle_y^z + \langle \partial_y M_u^{(a)} - \partial_x M_v^{(a)} \rangle^z. \end{aligned} \tag{F 4}$$

Here the notation

$$\langle a \rangle^z = \frac{1}{h_2} \int_{-1}^{-h_1} a \mathrm{d}z \tag{F 5}$$

is used. Using (F 4) we rewrite (6.6) in the form:

$$\Pi_{T_1}^- + u_g^- \Pi_x^- + v_g^- \Pi_y^- = \langle \langle \partial_y M_u^{(a)} - \partial_x M_v^{(a)} \rangle^z \rangle + \langle NR \rangle, \tag{F 6}$$

where

$$\begin{aligned} NR = {} & -\frac{1}{h_2} \eta_0 \partial_z w_0^- |_{z=-h_1} + \frac{1}{h_2} (u_a^- \partial_x \eta_0 + v_a^- \partial_y \eta_0)_{z=-h_1} + \partial_y u_g^- \langle u_a^- \rangle_x^z \\ & + \partial_y v_g^- \langle u_a^- \rangle_y^z - \partial_x u_g^- \langle v_a^- \rangle_x^z - \partial_x v_g^- \langle v_a^- \rangle_y^z + \alpha \langle w_0^- \rangle_y^z. \end{aligned} \tag{F 7}$$

By virtue of (4.6*c*) and (5.36*b*), (5.37), (5.32), (5.33) we have:

$$\eta_{0s} = \eta_{0c} = 0, \tag{F 8}$$

therefore

$$\langle NR \rangle = 0. \tag{F 9}$$

Using (5.4*e*) one readily shows that

$$\langle M_u^{(a)} \rangle = \langle (u_a^{-2})_x + (u_a^- v_a^-)_y + (u_a^- w_a^-)_z \rangle, \tag{F 10a}$$
$$\langle M_v^{(a)} \rangle = \langle (u_a^- v_a^-)_x + (v_a^{-2})_y + (v_a^- w_a^-)_z \rangle. \tag{F 10b}$$

Averaging (F 10) over the lower layer depth and using (5.37) one obtains:

$$\langle \langle M_u^{(a)} \rangle^z \rangle = \langle \langle (u_a^{-2})_x + (u_a^- v_a^-)_y \rangle^z \rangle, \tag{F 11a}$$
$$\langle \langle M_v^{(a)} \rangle^z \rangle = \langle \langle (u_a^- v_a^-)_x + (v_a^{-2})_y \rangle^z \rangle. \tag{F 11b}$$

By virtue of (5.36*a*)

$$\langle u_a^{-2} \rangle = \langle v_a^{-2} \rangle = \tfrac{1}{2} |A|^2, \quad \langle u_a^- v_a^- \rangle = 0, \tag{F 12}$$

therefore

$$\langle \langle M_u^{(a)} \rangle^z \rangle = \tfrac{1}{2} \langle |A|^2 \rangle_x^z, \quad \langle \langle M_v^{(a)} \rangle^z \rangle = \tfrac{1}{2} \langle |A|^2 \rangle_y^z. \tag{F 13}$$

Thus

$$\langle \langle \partial_y M_u^{(a)} - \partial_x M_v^{(a)} \rangle^z \rangle = 0 \tag{F 14}$$

and we arrive at (6.8*a*).

Appendix G. Some details of derivation of the amplitude equation

The only unknown function on the right-hand sides of (6.12) is the pressure $\tilde{p}_1$ which is found from (4.7*c*). Representing this equation in the form:

$$p_{1z} = \alpha(\langle u_0\rangle^z + \tilde{u}_a), \quad \langle u_0\rangle^z = u_g + \langle u_a\rangle^z, \tag{G 1a,b}$$

one readily shows that:

$$p_1 = \langle p_1\rangle^z + \tilde{p}_1, \tag{G 2}$$

where

$$\tilde{p}_1 = \alpha\left[\langle u_0\rangle^z(z+1-h_2/2) + \int_{-1}^{z}\tilde{u}_a\mathrm{d}z + \langle z\tilde{u}_a\rangle^z\right], \tag{G 3}$$

and the averaged $\langle p_1\rangle^z$ is a depth-independent function. Furthermore, it follows from (5.36*b*), (5.37) that:

$$\tilde{w}_0 = w_a - \langle w_a\rangle^z = -\frac{1}{2}\left[\mathrm{e}^{-\mathrm{i}t}\left(\int_{-1}^{z} s(A)\mathrm{d}z + \langle zs(A)\rangle^z\right) + \text{c.c.}\right] - (\bar{\bar{u}}_x + \bar{\bar{v}}_y)\left(z+1-\frac{h_2}{2}\right). \tag{G 4}$$

Finally, up to non-resonance terms we have:

$$\tilde{M}_u = u_g\partial_x\tilde{u}_a + v_g\partial_y\tilde{u}_a + \tilde{u}_a\partial_x u_g + \tilde{v}_a\partial_y u_g, \tag{G 5a}$$

$$\tilde{M}_v = u_g\partial_x\tilde{v}_a + v_g\partial_y\tilde{v}_a + \tilde{u}_a\partial_x v_g + \tilde{v}_a\partial_y v_g, \tag{G 5b}$$

i.e. (see (6.14) and (3.21*a,b*))

$$\tilde{M}_u + \mathrm{i}\tilde{M}_v = J(p_g, \tilde{U}_a) + \frac{\mathrm{i}}{2}\nabla_h^2 p_g\tilde{U}_a. \tag{G 6}$$

REFERENCES

BADULIN, S. I., VASILENKO, V. M. & YAREMCHUK, M. I. 1991 Interpretation of quasi-inertial motions using Megapoligon data as an example. *Izv. Atmos. Ocean. Phys.* **27**, 446–452.

BREKHOVSKIKH, L. M. & GONCHAROV, V. 1994 *Mechanics of Continua and Wave Dynamics*, 342 pp. Springer.

GERKEMA, T. & SHRIRA, V. I. 2005 Near-inertial waves in the ocean: beyond the traditional approximation. *J. Fluid Mech.* **529**, 195–219.

GERKEMA, T., ZIMMERMAN, J. T. F., MAAS, L. R. M. & VAN HAREN, H. 2008 Geophysical and astrophysical fluid dynamics beyond the 'traditional approximation'. *Rev. Geophys.* **46**, RG2004.

VAN HAREN, H. & MILLOT, C. 2005 Gyroscopic waves in the Mediterranean Sea. *Geophys. Res. Lett.* **32**, L24614.

IL'IN, A. M. 1970 Asymptotic properties of a solution of a boundary-value problem. *Math. Notes* **8**, 625–632.

IL'IN, A. M. 1972 On the behaviour of the solution of a boundary-value problem when $t\to\infty$. *Math. USSR, Sb.* **16**, 545–572.

KAMENKOVICH, V. M. 1977 *Fundamentals of Ocean Dynamics*, 249 pp. Elsevier.

KAMENKOVICH, V. M. & KAMENKOVICH, I. V. 1993 On the evolution of Rossby waves, generated by wind stress in a closed basin, incorporating total mass conservation. *Dyn. Atmos. Oceans* **18**, 67–103.

KAMKE, E. 1976 *Handbook of Ordinary Differential Equations*. Chelsea.

KASAHARA, A. 2003 The roles of the horizontal component of the Earth's angular velocity in nonhydrostatic linear models. *J. Atmos. Sci.* **60**, 1085–1095.

KOCHIN, N. E., KIBEL, L. A. & ROSE, N. V. 1964 *Theoretical Hydromechanics*. Wiley-Interscience.

LEBLOND, P. H. & MYSAK, L. A. 1978 *Waves in the Ocean*, 602 pp. Elsevier.

MIROPOL'SKY, Y. Z. 2001 *Dynamics of Internal Gravity Waves in the Ocean*, 406 pp. Kluwer.

PEDLOSKY, J. 1979 *Geophysical Fluid Dynamics*, 624 pp. Springer.

REZNIK, G. M. 2013 Linear dynamics of a stably-neutrally stratified ocean. *J. Mar. Res.* **71** (4), 253–288.

REZNIK, G. M. 2014 Geostrophic adjustment with gyroscopic waves: barotropic fluid without traditional approximation. *J. Fluid Mech.* **743**, 585–605.

REZNIK, G. M., ZEITLIN, V. & BEN JELLOUL, M. 2001 Nonlinear theory of geostrophic adjustment. Part 1. Rotating shallow-water model. *J. Fluid Mech.* **445**, 93–120.

SEDOV, L. I. 1997 *Mechanics of Continuous Media*, Series in Theoretical and Applied Mechanics, vol. 4. 1368 pp. World Scientific.

SHRIRA, V. I. & TOWNSEND, W. A. 2010 Inertia-gravity waves beyond the inertial latitude. Part 1. Inviscid singular focusing. *J. Fluid Mech.* **664**, 478–509.

SHRIRA, V. I. & TOWNSEND, W. A. 2013 Near-inertial waves and deep ocean mixing. *Phys. Scr.* **T155**, 1–12.

TIMMERMANS, M. L., MELLING, H. & RAINVILLE, L. 2007 Dynamics in the Deep Canada Basin, Arctic Ocean, inferred by thermistor chain time series. *J. Phys. Oceanogr.* **37**, 1066–1076.

YOUNG, W. R. & BEN JELLOUL, M. 1997 Propagation of near-inertial oscillations through a geostrophic flow. *J. Mar. Res.* **55**, 735–766.

ZEITLIN, V., REZNIK, G. M. & BEN JELLOUL, M. 2003 Nonlinear theory of geostrophic adjustment. Part 2. Two-layer and continuously stratified primitive equations. *J. Fluid Mech.* **491**, 207–228.